REVIEW ARTICLE

Acyclic oligopyrroles as building blocks of supramolecular assemblies

Hiromitsu Maeda

Abstract The supramolecular chemistry of acyclic oligopyrrole derivatives mainly reported by the author's group in the last four years has been summarized in this review. The author has demonstrated the "first step" to construct the new materials and concepts based on the new molecular systems consisting of pyrrole rings, which form the complexes, assemblies, and organized structures, by using noncovalent interactions such as metal coordination, hydrogen bonding, and π–π interaction. Acyclic π-conjugated oligopyrroles have exhibited not only host–guest binding behaviors in solutions but also the formation of, for example, (i) metal coordination polymers to give emissive colloidal spheres, (ii) solid-state assemblies of acyclic π-conjugated anion receptors and their anion complexes, (iii) anion-responsive supramolecular gels from the receptors with aliphatic chains, and (iv) solvent-assisted organized structures like vesicles derived from amphiphilic anion receptors.

Keywords Hydrogen bonding · Metal coordination · π-Conjugated system · Pyrrole · Supramolecular chemistry

Introduction

Pyrrole is well known as a π-conjugated aromatic heterocyclic molecule [1] comprising not only biotic dyes such as heme and chlorophyll but also artificial porphyrin derivatives [2]. In contrast to relatively "inert" benzene, pyrrole has excess electrons (six) as compared to the number of atoms (five) in the framework. Therefore, pyrrole moieties are reactive and stabilized by, for example, incorporation into the aromatic macrocycles such as porphyrins or substitution by electron-withdrawing moieties. Pyrrole exhibits "duality" of its nitrogen moiety, which behaves both as a hydrogen-bonding acceptor or metal coordination ligand due to the N site (Fig. 1a) and a hydrogen-bonding donor due to the NH site (Fig. 1b). As the π-planes of the pyrrole unit also enable effective interactions that yield stacking assemblies and metal complexes as π-ligands (Fig. 1c), pyrrole rings can act as potential building subunits forming supramolecular nanoscale structures. Well-defined organized architectures fabricated by self-assembled organic molecules have attracted considerable attention due to their ability to act as potential functional materials, that use noncovalent interactions such as metal coordination, hydrogen bonding, van der Waals interaction, etc. [3–8]. However, pyrrole rings are often observed as the components of the preorganized macrocycles, porphyrins and their analogs, wherein pyrrole N sites are faced to the inside of fairly rigid closed rings and consequently cannot exhibit their potential as interaction sites. Therefore, new aspects of pyrrole rings can be revealed by the synthesis of new oligopyrrolic systems to form functional supramolecular materials and construct new properties and concepts. This review comprises three main sections for the supramolecular chemistry of acyclic oligopyrroles: (i) metal-coordinated nanostructures (Sect. "Metal coordination of acyclic oligopyrroles"), (ii) solid-state hydrogen-bonding assemblies (Sect. "Hydrogen-bonding assembly of acyclic oligopyrroles"), and (iii) anion-binding receptors and their organized materials (Sect. "Supramolecular chemistry of

H. Maeda (✉)
College of Pharmaceutical Sciences, Institute of Science and Engineering, Ritsumeikan University, Kusatsu 525-8577, Japan
e-mail: maedahir@ph.ritsumei.ac.jp

H. Maeda
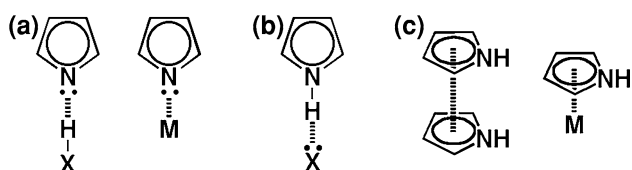PRESTO, Japan Science and Technology Agency (JST), Kawaguchi 332-0012, Japan

Fig. 1 Possible interactions of pyrrole as (**a**) a hydrogen-bonding acceptor and a metal coordination site, (**b**) a hydrogen-bonding donor, and (**c**) a π-plane for stacking and metal coordination. The structures with "aromatic circle" are used to represent various types of pyrrole units

acyclic oligopyrroles as anion-binding receptors"); these sections include the respective introduction parts. In the following sections, the author introduces the oligopyrrolic systems as the building units of the supramolecular assemblies reported by the author's group in the last four years [9] along with several examples reported by other groups.

Metal coordination of acyclic oligopyrroles

Metal coordination enables organic ligands to form versatile discrete or infinite architectures such as wire structures and nanospace materials, with potential applications in catalysis, optics, and biosensing [10–15]. However, metal-coordinated self-assemblies have thus far been limited to crystalline systems, which can enable the encapsulation of gas molecules in nanospaces. Recently, nanoscale morphologies based on coordination polymers existing as spherical and fibrous structures have been reported [16–18]. On the other hand, discrete coordination macrocycles and cages have also been investigated as isolated spaces to bind specific molecules and ions in solution. With regard to coordinating ligands, dipyrrins (dipyrromethenes)—considered as partial structures of bile pigments consisting of two pyrroles with an sp²-*meso* position—are essential π-conjugated bidentate monoanionic ligands for metal ions in natural and artificial systems [19–29]. Multitopic dipyrrin derivatives are promising scaffolds for self-assemblies and would provide neutral coordination polymers and oligomers, which, along with various spacer units, can be used to fabricate supramolecular structures and fine-tuned nanoscale morphologies by means of bridging the metal cations. For example, Cohen et al. showed infinite coordination networks based on dipyrrin derivatives in the solid state (Fig. 2a) [26–28]. Lindsey et al. reported dipyrrin metal complexes as bridging units for energy transfer systems consisting of porphyrins (Fig. 2b) [29]. Apart from these studies, the author has also attempted to form coordination polymers to yield nanoscale spherical architectures and discrete coordination macrocycles by using dimeric dipyrrin derivatives [30–34]. As an example,
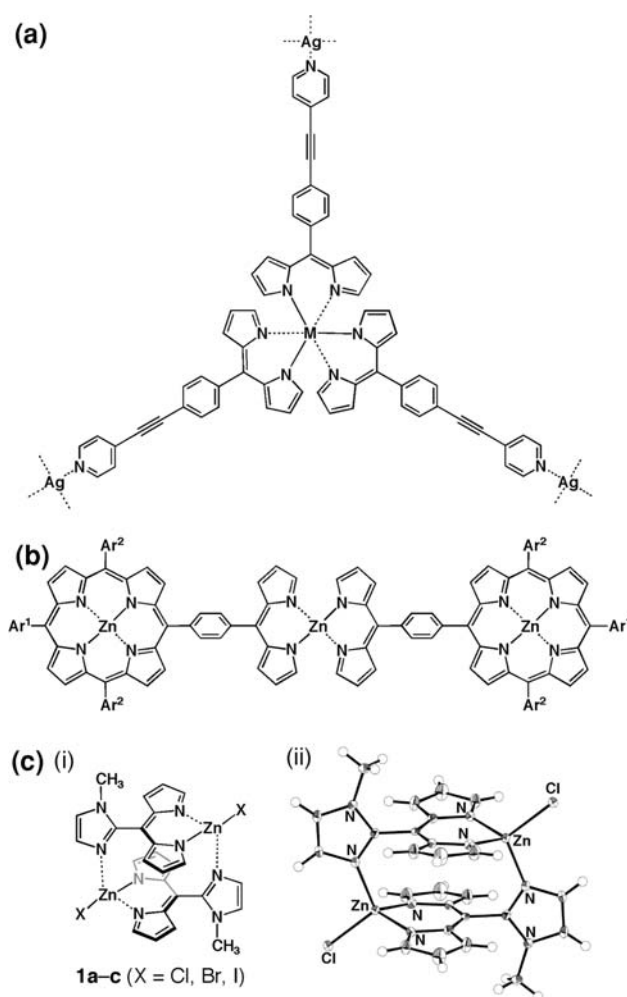

Fig. 2 Metal-coordination assemblies of dipyrrin derivatives: (**a**) infinite coordination networks based on dipyrrin derivatives; (**b**) porphyrin dimer bridged by dipyrrin-Zn^II complex; (**c**) (i) Zn^II-coordinated face-to-face dipyrrin dimers **1a–c** and (ii) ORTEP drawing (50% probability ellipsoids) of **1a** (CCDC#: 671563)

imidazolyl-substituted dipyrrin derivative forms the Zn^II-coordinated face-to-face stacking dimers **1a–c** (Fig. 2c(i)) by means of zinc halides, whose structure has been elucidated using single-crystal X-ray analysis (Fig. 2c(ii)) [30].

Nanoscale spherical architectures fabricated by metal coordination of multiple dipyrrin moieties

Based on the bis-dipyrrin derivatives bridged by a porphyrin unit as a spacer reported by the author's group [31], dipyrrin dimers (**2a–d**) with various rigid phenylethynyl spacers were prepared by performing the cross-coupling of bromobenzaldehydes and diethynylbenzenes, followed by condensation with pyrrole and subsequent DDQ oxidation. Dipyrrins **2a–d** were treated with 1 equiv. of Zn(OAc)₂ in THF to give polymeric structures (Fig. 3a), as confirmed by the UV/vis spectral changes in THF, ¹H NMR in

THF-d_8, and trace peaks of MALDI-TOF-MS. Self-assembled nanoscale structures of coordination polymers based on dipyrrin dimers were observed by using scanning electron microscopy (SEM), transmission electron microscopy (TEM), and optical microscopy (OM). Zinc(II) complexes of the rod-like *ppp* **2a** and crinkled *mmm* **2d** yield randomly shaped objects from THF, wherein the coordination polymer $2a_n \cdot Zn_n$ is less soluble and forms precipitates. In contrast, Zn^{II}-coordinated polymers of the partially crinkled *pmp* **2b** and *mpm* **2c** give uniform nanometer-sized spherical structures with diameters of ca. 300 nm from the same solvent with initial concentrations of ca. 10^{-3} M. Submicron-sized polymer particles are normally spherical in order to minimize the interfacial free energy between the particle and solvents. Further, dynamic light scattering (DLS) of $2b_n \cdot Zn_n$ and $2c_n \cdot Zn_n$ at 10^{-3} M in THF revealed the average diameter of their particles as ca. 100 nm, which suggests the formation of spherical structures in the solution. The effects of temperature, concentration, and solvents used were also observed. The metal-free dipyrrins **2a–d** give amorphous objects from THF, which suggest that the metal bridging between organic ligands as well as both *para* and *meta* linkages are required for well-defined nanoscale objects. As shown in Fig. 3b, object formation requires several steps: (i) formation of coordination polymers (primary), (ii) stacking of polymers (secondary), (iii) conversion into spheres (tertiary), and (iv) assembly into larger objects without fusion and segmentation (quaternary). The coordination polymers $(2b–d)_n \cdot Zn_n$ have emission maxima (λ_{em}) at 510–515 nm in THF (5×10^{-5} M), which can be ascribed to the Zn^{II}-bisdipyrrin moieties. The solid-state spherical objects obtained by the assemblies $(2b–d)_n \cdot Zn_n$ from THF give fluorescence at 532–543 nm. The coordination polymers of **2b** containing equivalent amounts of Zn^{II} and Cu^{II} ions formed in the THF solution result in the quenching of emission from the Zn^{II}-dipyrrin units possibly due to energy transfer [32].

Fig. 3 (**a**) Metal complexation of dipyrrin dimers **2a–d**; (**b**) formation pathway for particles from coordination polymers
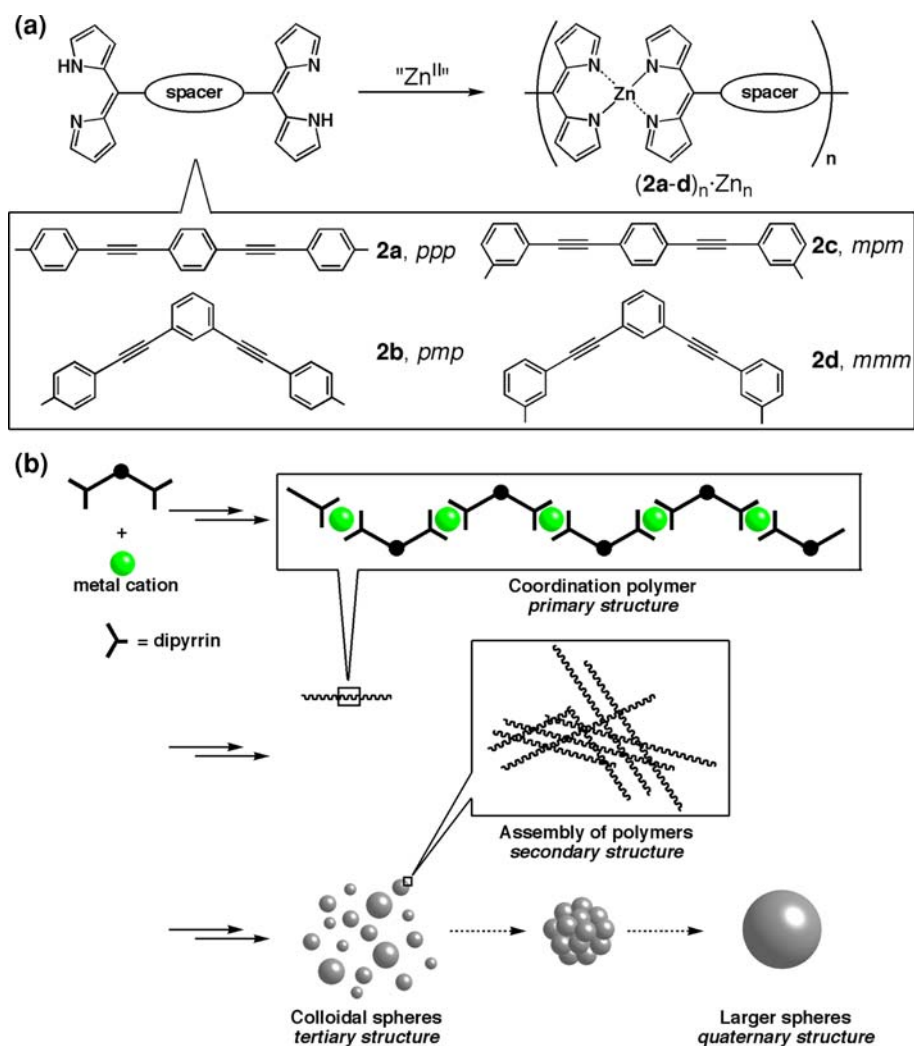
Nanoscale metal coordination macrocycles fabricated by dimeric dipyrrins

The treatment of **2d** with $Zn(OAc)_2$ and 0.5 equiv. of pyrene (with a length of ca. 9 Å) as a template molecule in $CHCl_3$ has afforded no higher homologs but discrete [2+2]-type coordination macrocycles, whose structures were initially revealed by ESI-TOF-MS analyses with $AgClO_4$ (5 equiv.) as a cation source associating the π-planes (Fig. 4a). The UV/vis absorption spectrum of $2d_2 \cdot Zn_2$ in $CHCl_3$ exhibits an absorption maximum (λ_{max}) at 486 nm, with a shoulder at ca. 465 nm, derived from a mixture of stereoisomers. In [2+2]-type complexes such as $2d_2 \cdot Zn_2$, two metal recognition sites (dipyrrin groups) are "strapped on" by phenylethynyl linkers; therefore, Zn^{II} complexes are classified into three types of stereoisomers (two diastereomers), namely, achiral (meso, $\Lambda\Delta$) and chiral ($\Lambda\Lambda$ and $\Delta\Delta$) derived from the two chiral centers due to the tetrahedral geometry of the Zn^{II} ion. The solid-state structure of the meso-type diastereomer $2d_2 \cdot Zn_2$, the major stereoisomer with a ratio of 4.6:1 in $CDCl_3$ at r.t., has been revealed by X-ray diffraction
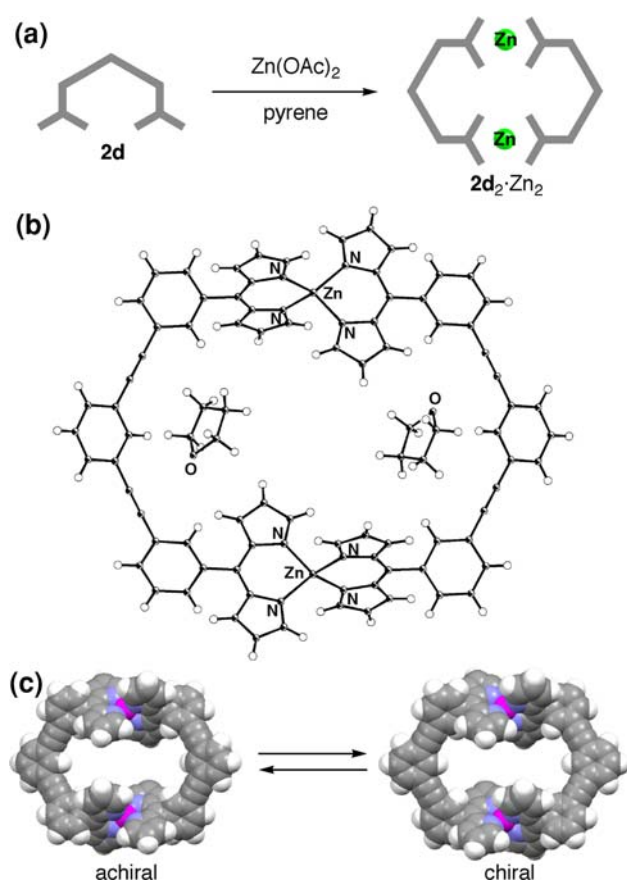

Fig. 4 (**a**) Formation of [2+2]-coordination macrocycle $2d_2 \cdot Zn_2$; (**b**) ORTEP drawing (50% probability ellipsoids) of $2d_2 \cdot Zn_2$ (achiral isomer) (CCDC# 635600); (**c**) transition between two stereoisomers

analysis using a single crystal from the mixture of the two diastereomers. The analysis shows a distorted hexagonal cavity with a diagonal of 1.6 nm encapsulating two THF molecules used as the solvent (Fig. 4b). From the equilibrium constants (K) between the chiral and meso isomers of $2d_2 \cdot Zn_2$ determined from the ^1H NMR spectra ($CDCl_3$) and the van 't Hoff plots, the thermodynamic parameters (ΔH^0, ΔS^0) could be estimated as 0.75 kJ/mol and 15 J/mol·K for $2d_2 \cdot Zn_2$; this suggests that the chiral isomer is slightly more thermodynamically stable than the achiral one. On the other hand, the rate constant (k) of the rotation of the dipyrrin moieties of $2d_2 \cdot Zn_2$ from the achiral to the chiral isomer has been determined to be 0.5 s^{-1} at 20 °C by means of the spin-saturation transfer method. Exchanges between the achiral and chiral isomers (Fig. 4c) would be achieved by the 90° rotation of one of the two dipyrrin-metal units, wherein one of the four β-CH units passes through a nanoscale ring cavity, such as those found in molecular motors or vehicles [33].

Hydrogen-bonding assembly of acyclic oligopyrroles

In natural systems, the double helix of DNA is constructed by complementary hydrogen bonding between the base pairs, and the high-dimensional structures of proteins are maintained by means of noncovalent interactions between the subunits such as amides [34]. At the same time, hydrogen-bonding interactions are useful to form various molecular assemblies and supramolecular structures in artificial systems [35–37]. Among the various ditopic interaction units, the set consisting of a pyrrole NH and hydrogen-bonding acceptor on the same plane would exhibit double hydrogen-bonding interactions that are appropriate for self-organization. Therefore, self-assembled supramolecular chain structures of the acyclic pyrrole derivatives with carbonyl groups at the α-positions have been observed in the solid state as well as in solution [38–43]. For example, bis(ethoxycarbonyl)-substituted terpyrrole and ferrocene-bridging pyrrole dimer form a 1D chain using N–H···O=C interactions in the solid state (Fig. 5a, b) [39, 41]. Recently, bis(iminopyrrole)benzenes have been reported to form nanostructural morphologies such as zigzag and straight chains depending on the isomers (Fig. 5c) [43]. However, micrometer- and nanometer-scale materials based on acyclic pyrrole derivatives have not been reported. The 1,3-dipyrrolyl-1,3-propanedione derivatives (Fig. 5d), which were first reported by Oddo et al. in the early twentieth century [44, 45], have yielded dimension-controlled micrometer- and nanometer-scale structures based on the hydrogen-bonding interactions of N–H···O = C [46]. Furthermore, the positions of the N site in meso-pyridyl-substituted dipyrromethanes affect the
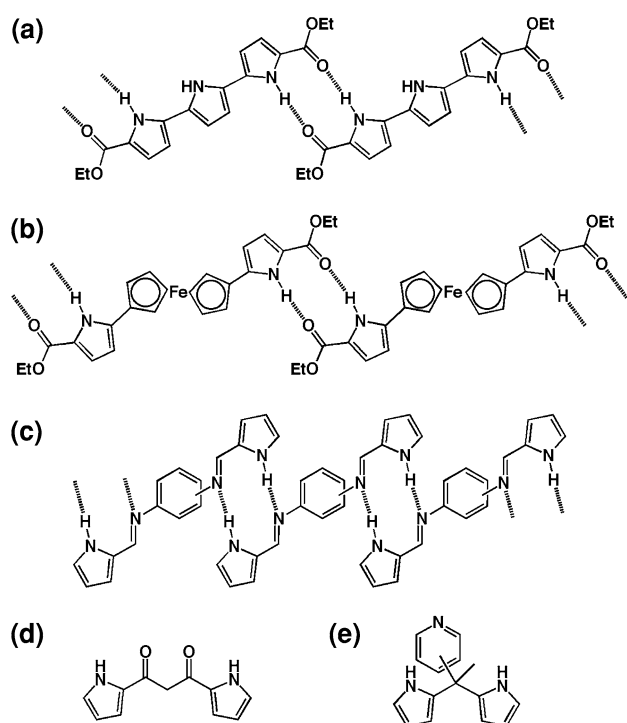
Fig. 5 (**a–c**) Hydrogen-bonding assemblies of pyrrole derivatives; (**d, e**) structures of 1,3-dipyrrolyl-1,3-propanedione and *meso*-pyridyl-substituted dipyrromethanes

structures of the molecular assemblies in the solid state (Fig. 5e) [47].

Micro- and nanometer-scale architectures fabricated from supramolecular assemblies of dipyrrolyldiketones

Various 1,3-dipyrrolyl-1,3-propanediones (**3a–e**, **4a–d**, **5a–d**, Fig. 6a) have been synthesized in modest yields from pyrroles and malonyl chloride derivatives in CH_2Cl_2 [44, 45]. In solution, dipyrrolyldiketones exist in equilibrium in a mixture with enol tautomers. Single-crystal X-ray analyses of dipyrrolyldiketones elucidated that the keto forms are more stable in the solid state. Further, unsubstituted **3a**, β-ethyl-substituted **3d**, and bridging-C-alkyl **5a** and **5b** form 1D intermolecular hydrogen-bonding assemblies using the NH and CO moieties at the edges of each molecule (Fig. 6b). Among these diketones, β-ethyl **3d** has a rather planar geometry that affords hydrogen-bonding arrays. In contrast, the N-methyl-substituted derivative (**5d**) exhibits a packing diagram without any hydrogen-bonding interactions in the solid state.

Various self-organizations of diketones observed in the X-ray structures enable the fabrication of micrometer- and nanometer-sized objects that are identifiable by SEM, TEM, and OM. From CH_2Cl_2, the objects were rapidly fabricated by solvent evaporation. In contrast to the

unsubstituted **3a** and methyl-substituted **3b** with rather crystalline flower-like and plate morphologies, respectively, the neopentyl-substituted derivative **3c** exhibits hexagonal tubes with pores having diagonals of 0.5–4 μm and lengths of 10–20 μm when the same solvent is used (Fig. 6d(i)). Smaller objects are also grown within some of the porous spaces (inset of Fig. 6d(i)). Similarly, β-ethyl-substituted **3d** forms tube structures with rectangle- and parallelogram-shaped pores with diagonals of 1–4 μm (Fig. 6d(ii)). On the other hand, β-fluorinated **3e** forms fibers with widths of 0.1–0.3 μm (Fig. 6d(iii)). Further, derivatives with long alkyl chains, such as hexadecyl substituents (**4d**), exhibit assemblies of thin-layered stacking sheets from CH_2Cl_2 (Fig. 6d(iv)). On the other hand, micro- and nanometer-scale objects such as sheets of alkyl-substituted derivatives **4a–d** are constructed in the solvent from hexane. Polymorphs from CH_2Cl_2, where the diketone derivatives are soluble as monomers, are fabricated during rapid solvent evaporation on the substrate to produce microcrystals (hexagonal and parallelogram tubes) or regularly ordered assemblies (fibers and sheets). Adequate alkyl chains or substituents are effective in the fabrication of micrometer- and nanometer-scale polymorphs controlled by the van der Waals interactions. The morphologies can be correlated with and explained by X-ray diffraction (XRD) analyses to show the existence of well-organized 2D lamellar multilayer structures in the cases of **4a–d** [46].

Hydrogen-bonding self-assemblies of *meso*-pyridyl-substituted dipyrromethanes

The self-assembled nanostructures of pyridyl-substituted dipyrromethanes **6a–c** (Fig. 7a) obtained by hydrogen bonding between the pyrrole NH and pyridyl N were examined by single-crystal X-ray analyses; for these analyses, the crystals are grown from CH_2Cl_2/hexane. 4-Pyridyl **6a** and 3-pyridyl-dipyrromethane **6b** form crinkled hydrogen-bonding chains and a dimeric structure, respectively (Fig. 7b(ii)). On the other hand, the 2-pyridyl isomer **6c** exhibited cyclic hexamers possessing hexagonal structures, each with a diagonal of 1.7 nm and height of 1.1 nm, because of the external N–H···N interactions as well as internal ones between NH and neighboring pyrrole π-planes (Fig. 7b(iii)). Moreover, columnar wires consisting of stacked cyclic hexamers were observed along the *c*-axis. Furthermore, in sharp contrast to *meso*-quaternary **6c**, *meso*-tertiary derivative **6c′** formed crinkled 1D chains similar to **6a**, implying that the substituents at the *meso* position also significantly affect the morphologies of nanostructures. Although the cyclic oligomers of pyrrole are the most stable species, also supported by the density functional

Fig. 6 (**a**) Dipyrrolyldiketone derivatives **3–5**; (**b**) hydrogen-bonding chains of (i) **3a**, (ii) **3d**, (iii) **5a**, and (iv) **5b** (CCDC#: 297709 (**3a**), 626137 (**3d**), 297710 (**5a**), 297711 (**5b**)); (**c**) SEM images of (i) **3c** and hexagonal pore (inset), (ii) **3d**, (iii) **3e**, and (iv) **4d** and assemblies of nanosheets (inset). The samples are prepared by casting of the CH$_2$Cl$_2$ solution on silicon substrate
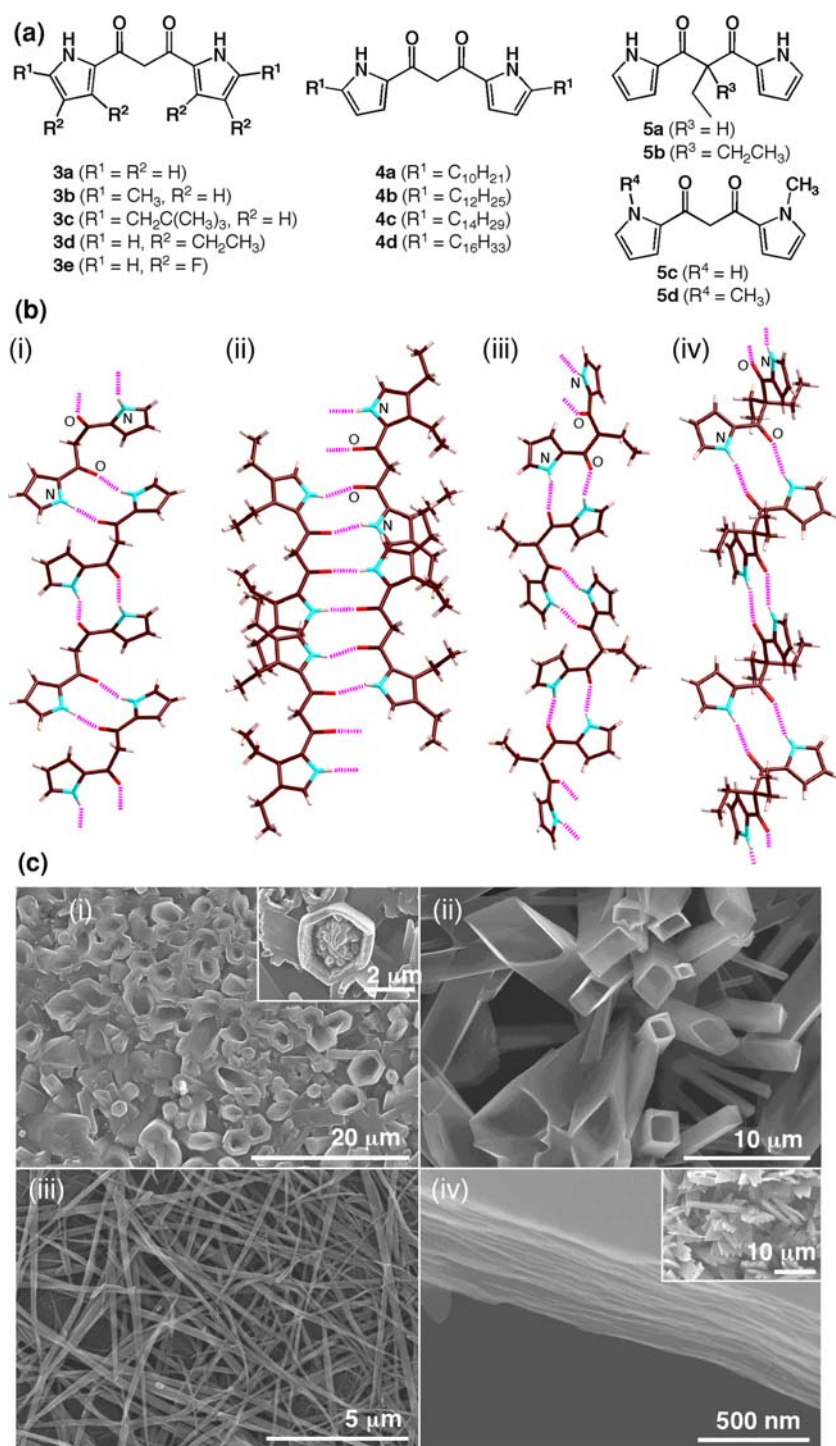
theory (DFT) calculations, and utilize all the NH sites during hydrogen bonding, cyclic hexamers have not been fabricated and observed thus far. ^{1}H NMR and DLS measurements indicate that dipyrromethanes **6a–c** exist as monomers in the solution state and form hydrogen-bonding assemblies in the solid state as a result of multiple weak interactions such as the van der Waals interactions [47].

Supramolecular chemistry of acyclic oligopyrroles as anion-binding receptors

Hydrogen-bonding interactions are useful for their association with specific guest species. Among the various "targets," the recognition of inorganic and biotic anions such as acetate, phosphate, and halide, which are ubiquitous in biology, is concerned with essential aspects such
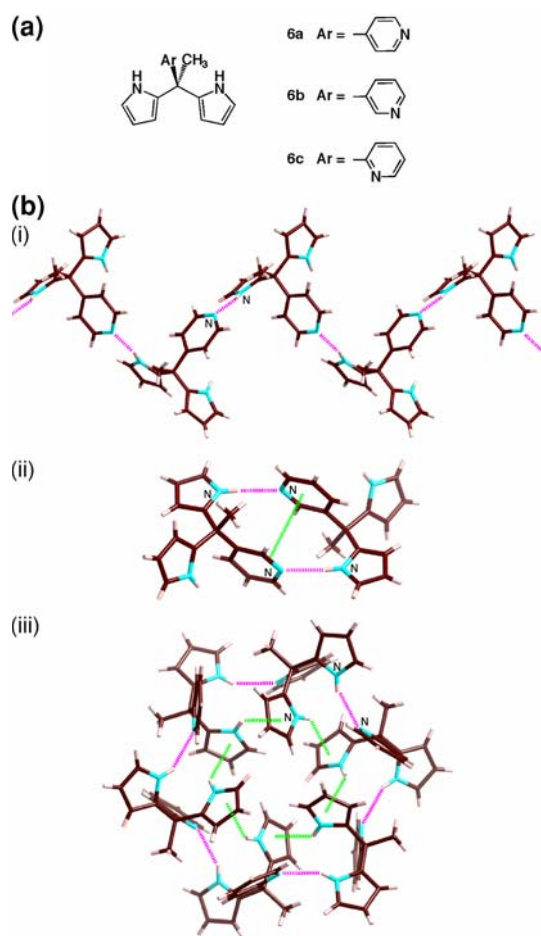
Fig. 7 (a) *meso*-Pyridyl-substituted dipyrromethanes **6a–c**; (b) solid-state hydrogen-bonding assemblies of **6a–c**. CCDC#: 637498 (**6a**), 637499 (**6b**), 637500 (**6c**)

as the activity of enzymes, transport of hormones, protein synthesis, and DNA regulation [48–57]. As an example, the antibiotic ristocetin has been known to efficiently and selectively bind amino acid carboxylates [58, 59]. At the same time, considerable efforts have been devoted to the development of artificial acetate ($CH_3CO_2^-$) and carboxylate receptors and carriers, and various binding motifs have been synthesized in recent years [60–62]. Further, anion complexes consisting of electronically neutral planar receptors and halide anions would afford "planar anions," which will be the essential building units for supramolecular assemblies and functional materials by the combination with appropriate counter cations.

Among the various artificial host molecules reported thus far, macrocycles consisting of pyrroles are particularly attractive because they behave as essential binding units due to the presence of polarized NH sites, as seen in di-protonated sapphyrins [63–65] and calixpyrroles [66–68] (Fig. 8a). Although less extensively studied, acyclic pyrrole derivatives have potentially even greater advantages

[56]. This is because they can form complexes with anions via the synthetic attachment of additional recognition units such as amide NH, or simply because they easily form macrocyclic systems. As targets by conformational changes, receptors with linear geometries are required to fit with the volume and shape of the negatively charged species. Therefore, in these cases, the essential factors that determine the binding affinities for guest species would be the existence of temporal preorganization, the strength of the induced effect required to polarize the association site(s), and the sterical and electrostatic repulsions by the peripheral substituents. Among the open-chain pyrrolyl anion receptors, the ones that have been reported are dipyrrol-ylquinoxalines as fluorescent dyes directly connected to pyrrole rings (Fig. 8b). These receptors undergo the quenching of emission in the presence of certain anions [69–71]. 1,3-Bis(pyrrol-2-yl)benzene, which is an essential building unit of macrocycles, has exhibited anion binding behaviors (Fig. 8c) [72]. Furthermore, amino acid bindings have been achieved by using synthetic receptors, such as amide- and guanidiniocarbonyl-substituted pyrroles (Fig. 8d) and pyrrole-based open-chain metal complexes [73–77]. A new set of acyclic oligopyrrole receptors based
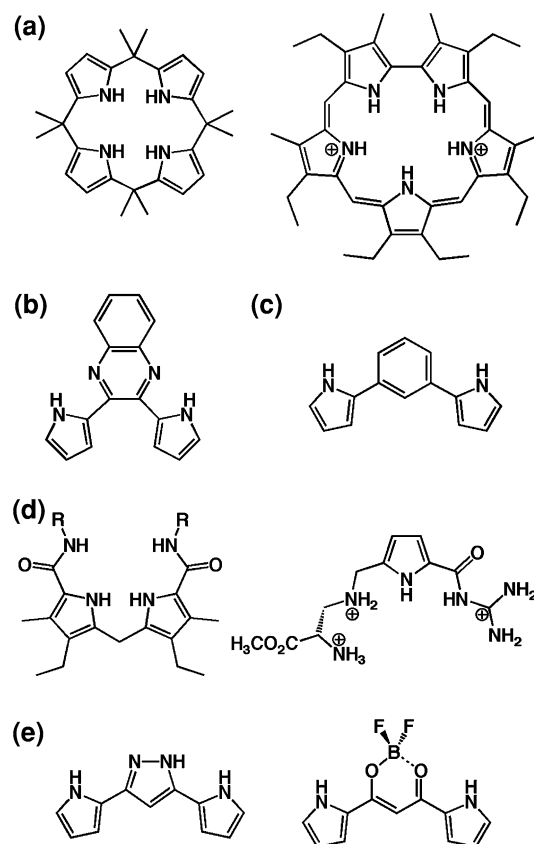

Fig. 8 Representatives of (**a**) cyclic and (**b–e**) acyclic oligopyrrole-based anion receptors

on 1,3-dipyrrolyl-1,3-propanediones (dipyrrolyldiketones), dipyrrolyl-substituted pyrazoles [78] and boron complexes (Fig. 8e) [79–92], have been synthesized; they act as building units of [2+2] assemblies to form micrometer- and nanometer-scale architectures and also as efficient colorimetric and fluorescent anion sensors to form supramolecular assemblies.

Dipyrrolylpyrazoles as anion receptors in protonated form and efficient building blocks for organized structures

Pyrazoles can interact electrostatically or via hydrogen bonds with anionic or polar substrates in partly or fully protonated forms. Therefore, the combination of pyrrole and pyrazole groups within a single molecule could yield an essential role for binding various guest species. In accordance with the first example reported by Oddo [44], dipyrrolylpyrazoles (*dpp*, **7a–e**, Fig. 9a) were synthesized by the condensation of excess hydrazine monohydrate with the corresponding dipyrrolyldiketones (**3a–c**, **4d**, **3e**) [28, 80, 82] in refluxing AcOH for 3–4 days. N-methyl-substituted **8a–c** were obtained similarly from diketone **5d** (for **8a**) or from the methylation of **7a** and **7e** (for **8b** and **8c**, respectively). The anion-binding ability of the pyrrole NH sites (e.g., binding constants (K_a) of **8b** and **8c** for $CH_3CO_2^-$ in CH_2Cl_2 are 1,600 and 28,000 M^{-1}, respectively) drove us to further investigate the details of *dpp* as a new class of π-conjugated systems. In fact, the planar [2+2]-binding structures of N-free *dpp* with TFA were elucidated by the X-ray analyses of **7a**$_2$ · TFA$_2$, **7b**$_2$ · TFA$_2$, and **7e**$_2$ · TFA$_2$ complexes (Fig. 9b). Among the anion-binding c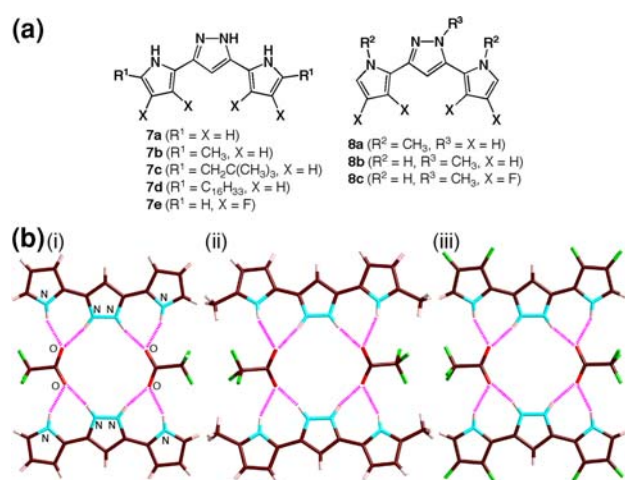omplexes [52–59], only a few examples of discrete aggregates consisting of multiple host and guest species have been reported [93–99]. By casting the TFA complexes of *dpp* in CH_2Cl_2 on a silicon substrate, organized structures have been observed by SEM analysis. In sharp contrast to unsubstituted **7a**$_2$ · TFA$_2$ and α-methyl **7b**$_2$ · TFA$_2$ that yield crystalline objects, TFA complexes **7c**$_2$ · TFA$_2$ and **7d**$_2$ · TFA$_2$ with neopentyl and hexadecyl chains provide petal-like objects with widths of ca. 500 nm and assembled sheet structures with thickness <100 nm. Further, β-fluorinated **7e**$_2$ · TFA$_2$ exhibits rod-like morphologies with widths of ca. 100–200 nm, as well as small amounts of microcrystals. On the other hand, the TFA complexes of N-blocked **8a** and **8b** as well as those of anion-free **7b–d** show only random and amorphous structures. Complexation with an acid would provide the planar geometry of *dpp*, which is required for the formation of micrometer- and nanometer-scale morphologies using intermolecular interactions such as π–π stacking [78].

Boron complexes of dipyrrolyldiketones as new class of acyclic anion receptors with planar geometries

In 2005, the author's group reported the BF$_2$ complex (**9a**, Fig. 10a) of dipyrrolyldiketone **3a** as a π-conjugated acyclic anion receptor by using pyrrole NH and bridging CH to afford a planar receptor–anion complex (Fig. 10b) [79]. The BF$_2$ complex **9a**, which exhibits pyrrole inversions in order to the bind the anion, can be considered as a "molecular flipper" to enable the space control between two planar states (free receptor and receptor–anion complex) by external chemical stimuli (anion). NH···X$^-$ and bridging CH···X$^-$ interactions are suggested by the ^{1}H NMR chemical shifts of **9a** in CD$_2$Cl$_2$ upon the addition of

Fig. 9 (**a**) Dipyrrolylpyrazoles **7a–e** and **8a–c**; (**b**) solid-state [2+2] assemblies of (i) **7a**$_2$ · TFA$_2$, (ii) **7b**$_2$ · TFA$_2$, and (iii) **7e**$_2$ · TFA$_2$. CCDC#: 625142 (**7a**$_2$ · TFA$_2$), 625143 (**7b**$_2$ · TFA$_2$), 625144 (**7e**$_2$ · TFA$_2$)
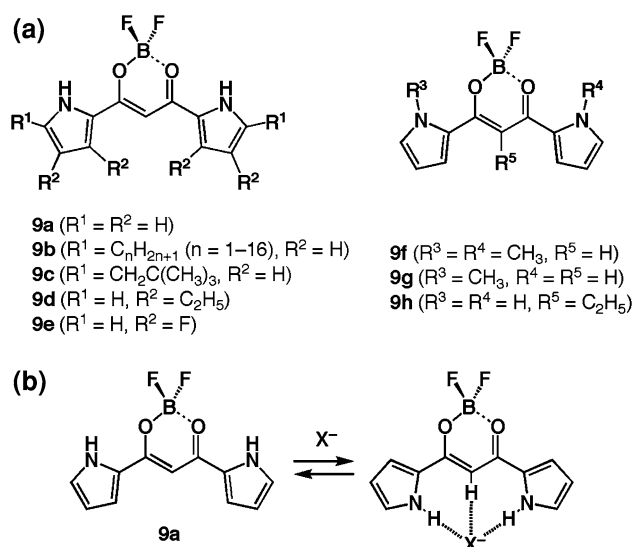

Fig. 10 (**a**) BF$_2$ complexes of dipyrrolyldiketones **9a–h**; (**b**) anion-binding mode of **9a**

anions as tetrabutylammonium (TBA) salts. Furthermore, the discrete resonances of the two species—free receptor and anion complex—suggest that the equilibrium between these forms is too slow to be detected in the NMR time-scale, possibly due to the requirement of pyrrole inversions to bind the anion. The absorption and emission maxima of the receptor **9a** are observed at 432 and 451 nm in CH_2Cl_2, respectively, which are adjusted by the addition of anions as TBA salts, suggesting its potentiality as a colorimetric anion sensor.

Pyrrole, a π-conjugated moiety composing the molecular flipper **9a**, can be transformed to various pyrrole derivatives due to the reactivity and selectivity [1]. Based on the library of pyrrole derivatives reported so far, the introduction of substituents to the receptor framework would yield the various molecular flippers with new electronic and photophysical properties. For example, we have synthesized the α-alkyl-substituted receptors **9b–n** and **9c** (Fig. 10a) from α-alkylpyrroles, which have revealed the behaviors that suggest that the binding constants are smaller in the receptors with longer alkyl chains and that binding kinetics are also dependent on the alkyl chain lengths [79, 80]. On the other hand, β-ethyl- and β-fluorine-substituted receptors **9d** and **9e** can be considered as building blocks to form the covalently linked oligomers due to the α-free positions [81, 82]. The anion-binding properties of the BF_2 complexes were examined by the UV/vis absorption spectral changes upon the addition of anions (Cl^-, Br^-, $CH_3CO_2^-$, $H_2PO_4^-$, and HSO_4^-) as TBA salts in CH_2Cl_2. The binding constants (K_a) of **9a**, **9b-16**, and **9c–e** are summarized in Table 1; enhanced values are obtained for unsubstituted **9a** due to less sterical hindrance at pyrrole α-positions along with β-fluorinated derivative **9e** due to the polarized NH and CH binding sites. The receptor **9a** has exhibited the efficient anion binding property compared to dipyrrolylquinoxaline [69] and 1,3-bis(pyrrol-2-yl)benzene (in CH_2ClCH_2Cl) [72]. All the receptors **9a–e** shown here bind $CH_3CO_2^-$ more efficiently than the other anions. Upon the addition of $CH_3CO_2^-$ to **9e** (2×10^{-3} M) in CD_2Cl_2 at –50 °C, both the NH and CH peaks (at 9.02 and 6.65 ppm, respectively) in ^1H NMR disappear and new signals appear in the downfield region at 12.09 and 8.23 ppm, respectively. Similar downfield shifts are observed upon the addition of other anions to these acyclic receptors. The anion-binding behaviors of the "blocked" derivatives (**9f–h**, Fig. 10a), which were synthesized from **5d**, **5c**, and **5a**, respectively, suggest the essential role of the bridging CH site for anion binding [83].

The above observations in which the anion-binding behaviors of these acyclic receptors can be correlated with the effects of the peripheral substituents can be explained by the DFT calculations at the B3LYP/6-31G(d,p) level. Consistent with the experimental results such as NMR, molecular simulations for the receptors **9a–e** have suggested that the most stable conformations of the free receptors with intramolecular interactions between pyrrole NH and oxygens (e.g., the left structure in Fig. 10b) are unsuitable for anion recognition and therefore pyrrole inversions are required to bind anions. The relative energies of the "preorganized" structures (e.g., the right structure in Fig. 10b) of **9a–e** compared to each stable conformation are estimated as 9.08, 9.10 (**9b-8** as an example), 8.96, 4.98, and 15.04 kcal/mol, respectively, suggesting that the β-ethyl-substituted receptor **9d** shows stronger preferred preorganized geometries than **9a–c** and **9e**. From the experimental and theoretical data, the affinities for anions can be determined from the following factors: (i) electronic effects of the peripheral substituents, (ii) sterical effects of the α-substituents, and (iii) relative stabilities of the preorganized conformation.

Aryl-substituted anion receptors and their covalently linked oligomers

In order to extend the π-conjugation of molecular flippers, we have attempted to synthesize α-aryl-substituted derivatives of BF_2 complexes. Initially, α-aryl-substituted **10a–d** (Fig. 11a) were obtained from the α-aryl-substituted pyrroles, which were synthesized by the cross-coupling reactions, via the corresponding α-aryl-substituted dipyrrolyldiketones. The absorption maxima (λ_{max}) of **10a**, **10b**, and **10d** in CH_2Cl_2 appear at 500, 480, and 516 nm in CH_2Cl_2, respectively, which are red-shifted as compared to

Table 1 Anion-binding constants (K_a, M^{-1}) of **9a**, **9b-16**, and **9c–e** upon the addition of anions as TBA salts in CH_2Cl_2

Anion	K_a (**9a**)	K_a (**9b-16**)	K_a (**9c**)	K_a (**9d**)	K_a (**9e**)
Cl^-	15,000	4,000 (0.27)	2,000 (0.13)	6,800 (0.45)	26,000 (1.73)
Br^-	2,100	680 (0.32)	330 (0.16)	1,200 (0.57)	1,700 (0.81)
$CH_3CO_2^-$	930,000	110,000 (0.12)	110,000 (0.12)	210,000 (0.23)	960,000 (1.03)
$H_2PO_4^-$	270,000	20,000 (0.07)	13,000 (0.048)	91,000 (0.34)	190,000 (0.70)
HSO_4^-	–	– (–)	80 (–)	1,200 (–)	1,100 (–)

The values in the parentheses are the ratios to the K_a values of **9a**

(a)

10a (R¹ = R² = R³ = H)
10b (R¹ = H, R² = CH₃, R³ = H)
10c (R¹ = R² = CH₃, R³ = H)
10d (R¹ = R² = H, R³ = OCH₃)

11a (R = I)
11b (R = C₆H₅)
11c (R = 2-pyrrolyl)
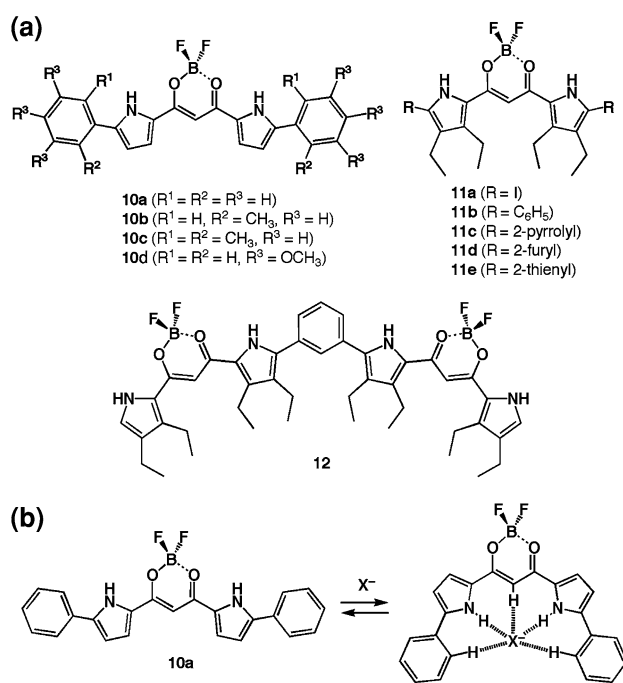11d (R = 2-furyl)
11e (R = 2-thienyl)

12

(b)

10a

Fig. 11 (**a**) Aryl-substituted derivatives **10a–d**, iodinated **11a**, β-ethyl-substituted aryl-substituted receptors **11b–e**, and phenylene-bridged dimer **12**; (**b**) anion-binding mode of aryl-substituted receptor **10a**

9a (432 nm), **9b-16** (457 nm), **9c** (457 nm), **9d** (452 nm), and **9e** (421 nm). Conversely, $\lambda_{\max}$ for **10c** appears at 456 nm, which is blue-shifted by 46, 24, and 60 nm as compared to **10a**, **10b**, and **10d**, respectively, as a result of the distortion of the aryl rings. The gaps between the HOMO and LUMO of these receptors (e.g., 3.084 eV for **10a**, 3.148 eV for **10b**, 3.385 eV for **10c**, 3.578 eV for **9a**, 3.431 eV for **9c**, and 3.470 eV for **9d**) are related to these electronic absorption bands [84, 85].

The synthetic route for **10a–d** based on aryl-substituted pyrroles is useful but applied to only a limited number of the derivatives. Therefore, the design of more efficient routes is required in order to introduce various aryl rings to the molecular flippers. In fact, selective iodination at the α-pyrrole positions of β-ethyl-substituted **9d** by treatment with 2.7 and 1.1 equivs. of N-iodosuccinimide (NIS) in CH₂Cl₂ is found to be a key procedure to afford mono-**11a′** and bisiodinated derivative **11a** as the essential starting materials of the coupling reactions for various utility molecules and covalently linked oligomer systems. Bromination by N-bromosuccinimide (NBS) gave complicated mixtures containing species with a bromo-substituent at the fairly reactive bridging carbon. Suzuki cross-coupling reactions of **11a** and phenylboronic acid (2.2 equiv.) afforded bisphenyl-substituted **11b**, while a similar procedure using monoiodinated derivative **11a′** and phenylboronic acid (1.2 equiv.) afforded monophenyl derivative **11b′** [86]. Under similar conditions using the

corresponding aryl boronic acids, the bisiodinated derivative **11a** can be transformed into pyrrolyl-, furyl-, and thienyl-substituted derivatives **11c–e** [87]. In fact, the UV/vis absorption bands of **11b–e** in CH₂Cl₂ are observed at 499, 551, 538, and 527 nm, respectively, suggesting red-shifts that are comparable to that of α-unsubstituted **9d** (451 nm). The order of these $\lambda_{\max}$ values is correlated to the HOMO-LUMO gaps (**11b**: 3.154 eV; **11c**: 2.814 eV; **11d**: 2.865 eV; **11e**: 2.923 eV; **9d**: 3.470 eV) estimated by the DFT calculations. The covalently linked dimer **12** has been synthesized by the coupling reaction of monoiodinated derivative **11a′** (2 equiv.) with 1,3-benzenediboronic acid bis(pinacol)ester. Further iodination of phenylene-bridging dimer **12** afforded bisiodinated and monoiodinated dimers using 2.3 and 1.0 equivs. of NIS, respectively. Dimer **12**, whose $\lambda_{\max}$ value is 489 nm due to the incomplete π-conjugation at the *meta*-phenylene linkage, and its their iodinated derivatives can be potential subunits to form anion-responsive oligomers [86].

The anion affinities of the aryl-substituted receptors **10a–c** and **11b–e** were estimated from the changes in the UV/vis absorption spectra in the presence of increasing concentrations of the respective anions (Tables 2, 3). Compared to unsubstituted **9a**, α-phenyl **10a** shows augmented K_a values, especially for halides (ca. 2.0 and 1.3 holds enhancement for Cl⁻ and Br⁻, respectively) possibly due to pentacoordination (Fig. 11b) in contrast to the oxoanion binding. In contrast, doubly and totally *o*-C-blocked **10b** and **10c** exhibit K_a values (ca. 1/10 and 1/15 for Cl⁻ binding) less than those of **10a** possibly due to sterical hindrance and electrostatic repulsion of the anions by the π-plane. Compared to **10a**, β-ethyl **11b** has shown similar and smaller K_a values for oxoanions and halides, respectively. Further, the K_a values of **11b–e** are determined by UV/vis absorption spectral changes induced by the addition of appropriate anions as TBA salts in CHCl₃ containing 0.5% EtOH, which suppresses the binding affinities due to the higher K_a values of **11c** in CH₂Cl₂. For example, pyrrolyl **11c** shows considerably larger K_a values, $>10^6$ M⁻¹ for Cl⁻, H₂PO₄⁻ and CH₃CO₂⁻, than **11a,d,e** and α-unsubstituted **9d** due to the presence of multiple polarized NH sites. ¹H NMR spectral changes of **10a–c** and **11b–e** by anions provided valuable insights into (i) the binding behaviors of aryl-CH (or NH for **11c**) along with those of core pyrrole NH and bridging CH and (ii) the possible binding modes. For example, upon the addition of 1.5 equiv. of Cl⁻ as a TBA salt to a CD₂Cl₂ solution of **10a** (1 × 10⁻³ M) at 20 °C, the signals due to **10a** at 7.68 (*o*-CH), 9.73 (pyrrole NH), and 6.23 (bridging CH) ppm decreased in intensity with the concurrent appearance of new signals at 8.19, 12.27, and 9.04 ppm, respectively [84]. Similarly, upon the addition of 1 equiv. of Cl⁻ to CDCl₃ solution of **11c** (1 × 10⁻³ M) at 20 °C, the signals

of the "inner" NH and "outer" (terminal) NH are shifted from 9.29 and 8.77 ppm to 11.04 and 11.16 ppm, respectively, suggesting that the anions are bound more tightly to the terminal pyrrole NH. Similar downfield shifts of o-CH or β-CH are observed in **11b,d,e**. Despite these results, α-aryl **11b,d,e** afford fairly smaller K_a values than α-unsubstituted **9d**, possibly due to distorted aryl rings formed by the sterical hindrance of proximal β-ethyl units [86, 87]. Further, the signals of the aryl-substituted receptors and the pentacoordinated receptor–anion complexes can be observed independently, suggesting that a slow exchange takes place between these species at the NMR time scale. Rate constants k for the F$^-$, Cl$^-$, and Br$^-$ binding of, for example, **10a** using TBA salts in CH$_2$Cl$_2$ at 25 °C have been estimated to be 7.2×10^4, 13.0×10^4, and 6.0×10^4 M^{-1} s^{-1}, respectively, by stopped-flow measurements [100, 101]. While the order of k (Cl$^-$ > Br$^-$) is consistent with that of the binding constants (K_a), the more associated F$^-$ (240,000 M^{-1}) exhibits an intermediate value between those of Cl$^-$ and Br$^-$; this suggests that thermodynamic stability is not always correlated with the kinetic properties [84].

Solid-state assemblies of acyclic anion receptors and their anion complexes

Solid-state assemblies of the acyclic anion receptors have been revealed by single-crystal X-ray analyses, wherein the pyrrole nitrogens face opposite sides of the molecule, possibly due to the intramolecular N–H···O interactions in the solid state (Fig. 12). Unsubstituted **9a** [79, 88], α-alkyl-substituted **9b-1,4**, **9c** [80, 83], and β-fluorinated **9e** [82] form slipped 1D stacking structures based on the core π-plane. α-Aryl-substituted **10a,b** form similar attacking assemblies, wherein the slightly distorted aryl rings in o-tolyl-substituted **10b** produce less-effective stacking, while 2,6-dimethylphenyl-substituted **10c** has shown no stacking structures due to sterical hindrance [84]. X-ray analysis of **10d** shows one trimeric and two tetrameric stacking structures as the various slipped assemblies in the solid state. In contrast, α-ethyl-substituted **9b-2** and β-ethyl-substituted **11a–e** form the dimer structures

regardless of whether α-aryl-moieties are attached or not [80, 86, 87, 89]. In most structures, through intermolecular N–H···F hydrogen bonds, complicated 3D networks are formed along with stacking interactions. For example, the receptors **10a,b** and **11a–e** form dimeric structures using N–H···F and aryl-C(N)–H···F interactions, while such assemblies are not formed for **10c,d**. Single-crystal X-ray diffraction analyses reveal that the weak interaction of o-CH, β-CH, or pyrrole NH should play the role of a ligand for the anions in the solution. As you can observe, the acyclic anion receptors exist as dispersed monomer forms in good solvents, while they form ordered 3D organized structures, crystals, in poor solvents. The author's group is investigating the photophysical and electric conductive properties of the single-crystal states, which would exhibit unique properties due to the ordered assembled structures consisting of π-conjugated molecules [88].

The solid-state structures of the receptor–anion complexes have also been revealed by single-crystal X-ray analyses (Fig. 13). The receptor–anion complexes are dispersed in good solvents and in some cases crystallized in poor solvents such as hydrocarbons to give single crystals obtained by using tetraalkylammonium salts of anions. In the case of the Cl$^-$ complex of unsubstituted **9a**, using a 1:1 mixture of the receptor and TBACl, the CH proton and one of the two pyrrole NH protons are associated with the Cl$^-$ anion. The other NH proton turns to the opposite side and binds to another Cl$^-$ anion to form an anion-bridging 1D hydrogen-bonding infinite chain (Fig. 13a) [79]. The β-fluorinated **9e** utilizes only the NH interaction site to form the supramolecular 1D chains bridged by Cl$^-$, possibly due to the more polarized NH as compared to those of the β-H derivative (Fig. 13b) [82]. In both cases, counter cations (TBA) are located between the 1D receptor–anion chains that are quite different from the binding modes in the solution state, to form alternatively stacked structures. In contrast to the α-unsubstituted **9a** and **9e**, α-ethyl **9b-2** has shown a similar binding mode as observed in the solution state with inversion of two pyrrole rings (Fig. 13c) [80]. Furthermore, the anion complexes of α-aryl-substituted receptors, **10a** · Cl$^-$, **10d** · Cl$^-$, and **11c** · Cl$^-$, form pentacoordinated geometries as the building components

Table 2 Anion-binding constants (K_a, M^{-1}) of **10a–c**, **11b**, and **9a** upon the addition of anions as TBA salts in CH$_2$Cl$_2$

Anion	K_a (**10a**)	K_a (**10b**)	K_a (**10c**)	K_a (**11b**)	K_a (**9a**)
Cl$^-$	30,000 (2.0)	2,500 (0.17)	1,000 (0.067)	6,800 (0.45)	15,000
Br$^-$	2,800 (1.3)	300 (0.14)	20 (0.0095)	1,200 (0.57)	2,100
CH$_3$CO$_2^-$	210,000 (0.23)	150,000 (0.16)	150 (0.00016)	210,000 (0.23)	930,000
H$_2$PO$_4^-$	72,000 (0.27)	8,000 (0.029)	1,400 (0.0052)	91,000 (0.34)	270,000
HSO$_4^-$	540 (–)	35 (–)	14 (–)	–	–

The values in the parentheses are the ratios to the K_a values of unsubstituted **9a**

Table 3 Anion-binding constants (K_a, M^{-1}) of **11b–e** and **9d** upon the addition of anions as TBA salts in 0.5% EtOH/CHCl$_3$

Anion	K_a (**11b**)	K_a (**11c**)	K_a (**11d**)	K_a (**11e**)	K_a (**9d**)
Cl$^-$	120 (0.12)	1,200,000 (1200)	360 (0.36)	1,100 (1.1)	990
Br$^-$	30 (0.18)	180,000 (1100)	68 (0.40)	150 (0.88)	170
CH$_3$CO$_2^-$	410 (0.076)	3,000,000 (560)	500 (0.093)	1,000 (0.19)	5,400
H$_2$PO$_4^-$	130 (0.0086)	1,800,000 (120)	810 (0.054)	880 (0.059)	15,000
HSO$_4^-$	3 (0.014)	170,000 (810)	180 (0.85)	15 (0.071)	210

The values in the parentheses are the ratios to the K_a values of β-ethyl-substituted **9d**. K_a values provided in Table 3 are those of solvated receptors, solvated anions, and receptor–anion complexes
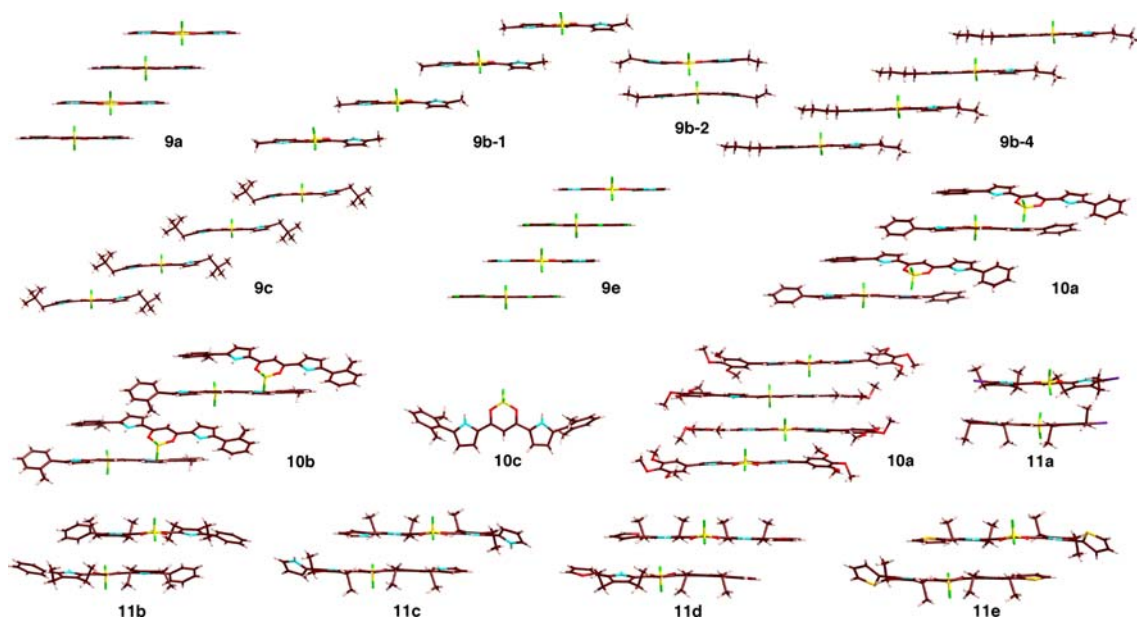

Fig. 12 Selected solid-state molecular assemblies of acyclic anion receptors. CCDC#: 270295 (**9a**), 666247 (**9b-1**), 666248 (**9b-2**), 666249 (**9b-4**), 288404 (**9c**), 290270 (**9e**), 639766 (**10a**), 639767 (**10b**), 639768 (**10c**), 639770 (**10d**), 680227 (**11a**), 680228 (**11b**), 585533 (**11c**), 585534 (**11d**), 585535 (**11e**)

of the electrostatically mediated alternatively stacking structures consisting of "planar anions (receptor–anion complexes)" and tetraalkylammonium cations (Fig. 13d–f) [84, 87]. Based on the "charge-by-charge" columnar structures, which are observed only in the crystal states as 3D organized structures at present, dimension-controlled organic salts can be fabricated by using planar anions under appropriate conditions.

Anion-responsive supramolecular gels consisting of acyclic anion receptors

π-Conjugated oligomers capable of guest binding are fascinating and potentially useful materials because of the possible solvent-free detection of analytes in the solid (i.e., film) state [102–104]. Apart from covalently linked oligomers, supramolecular assemblies assisted by noncovalent π–π interactions can be considered as stacking oligomers. Among the self-assembled oligomeric systems based on low-molecular-weight π-conjugated molecules, the gel materials—especially those susceptible to the influence of external stimuli—are of interest and play a crucial role as potential soft materials [105–114]. Supramolecular gels consist of nanoscale fibers, tubes, and sheets, formed by organized molecular assemblies. In contrast to physical stimuli, the structural modification of supramolecular organogels under chemical control is very attractive since a large variety of potential additives are available. Recently, the chemistry of anion-responsive supramolecular gels have attracted much attention due to their potentials as stimuli-responsive functional soft materials [115–128]. Some of the amide- and urea-based supramolecular gels are anion-responsive due to the affinities of polarized NH sites for anions that disrupt the hydrogen-bonding-assembled structures [116–124]. Further, supramolecular gels consisting of metal complexes also exhibit transformation by anions [125–128]. For example, Aida et al. reported an alkyl-substituted pyrazole-Au$^+$ trinuclear complex that
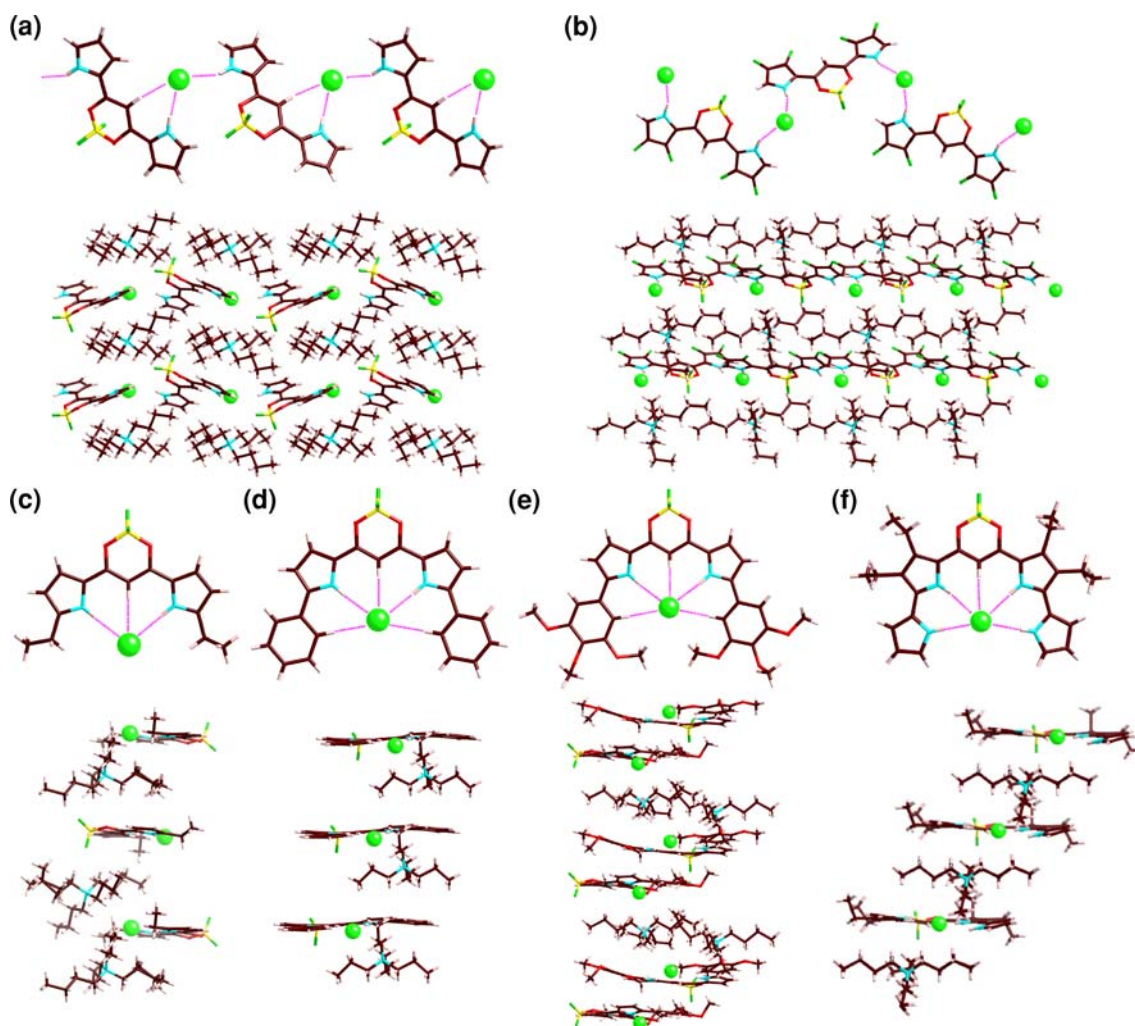
Fig. 13 Selected solid-state assemblies of receptor–anion complexes: (a) **9a** · Cl⁻; (b) **9e** · Cl⁻; (c) **9b-2** · Cl⁻; (d) **10a** · Cl⁻; (e) **10d** · Cl⁻; (f) **11c** · Cl⁻. Tetraalkylammonium cations are omitted for clarity in the top views. CCDC#: 270297 (**9a** · Cl⁻), 290271 (**9e** · Cl⁻), 666250 (**9b-2** · Cl⁻), 646480 (**10a** · Cl⁻), 639771 (**10d** · Cl⁻), 585536 (**11c** · Cl⁻)

forms a red-emissive supramolecular hexane gel, whose states and emission behaviors are controlled by the anion-driven "liberation" of metal ions [126]. Lee et al. prepared a dendrimer-like oxyethylene-substituted bispyridine derivative that forms coordination polymers or oligomers by Ag⁺ complexation, such as dispersed helical structures and discrete cyclic conformations; the morphologies of the organized structures depend on the coexisting counter anions such as NO₃⁻, BF₄⁻, and CF₃SO₃⁻ without specific interactions with the gelators [127, 128].

Porphyrins and related macrocycles are representatives of "extended" oligopyrroles; they can form self-assemblies by means of π–π-stacking interactions [2, 111, 112, 116]. Aryl-substitution at the pyrrole α-positions in the **10a–d** and **11b–e** systems enables various substituents to be introduced in this new class of acyclic anion receptors. Modification at the periphery of the receptors makes it possible to stabilize the stacking structures not only in the solid state but in the

solution state as well; for example, the introduction of various additional interaction moieties at the α-aryl rings enables the formation of molecular assemblies as soft matter that exhibit specific properties such as anion-responsive organized structures. Actually, the derivatives with aliphatic chains at the aryl rings (**13a–c**, Fig. 14a) have been obtained by similar procedures for **10a–d**. These anion receptors **13a–c** gelate octane (10 mg/mL); the transition temperatures between the gel and solution states have been found to be –8.5 (**13a**), 4.5 (**13b**), and 27.5 °C (**13c**), suggesting that the longer alkyl chains afford more stable gels. Octane gel of hexadecyloxy-substituted **13c** (10 mg/mL) exhibits split absorption bands with absorption maxima at 525 and 555 nm along with a shoulder at 470 nm; this is in contrast to the single peak at 493 nm exhibited in a diluted solution containing the dispersed monomers. This observation suggests that the gels are possibly derived from assemblies consisting of both H- and J-aggregates. The octane gel has
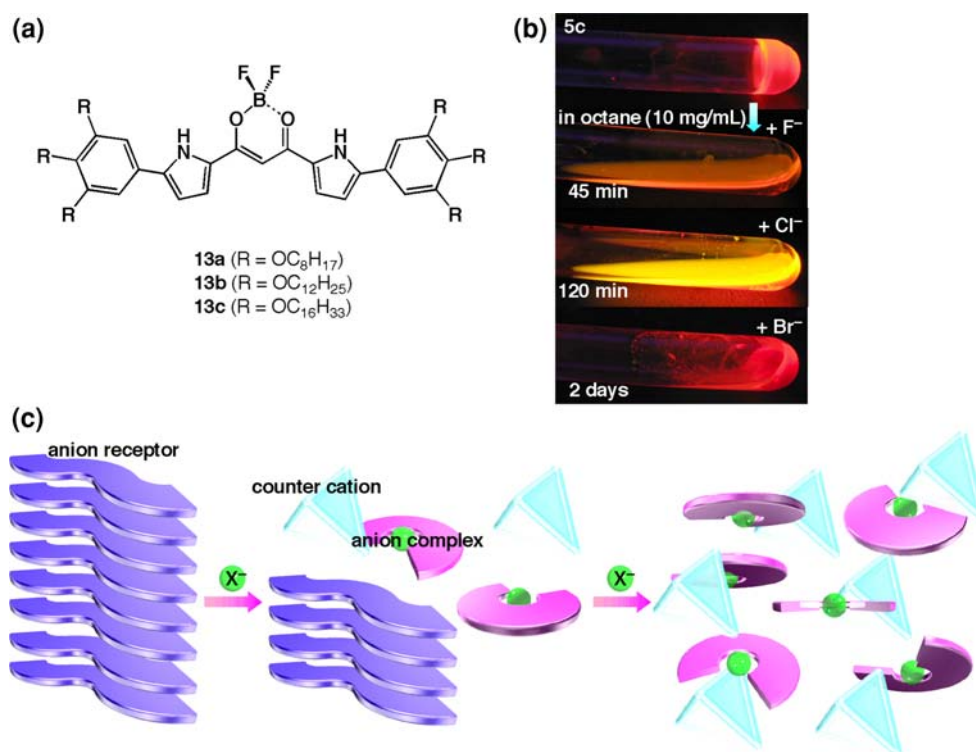
been found to exhibit emission at 654 nm (excited at 470 nm), which is red-shifted as compared to that ($\lambda_{em} = 533$ nm, $\lambda_{ex} = 493$ nm) in the diluted condition (1×10^{-5} M). Supramolecular organogel formation is achieved for the ordered structures based on the noncovalent interactions between the π-conjugated moieties and their substituents; this is supported by the atomic force microscopy (AFM), SEM, and XRD observations.

The addition of TBA salts of anions (10 equiv.) in the solid form to the fluorescent octane gel results in the transition to the solution state (Fig. 14b); the gels are gradually transformed into solutions beginning from areas close to where the solid salts have been added. The time required for complete transition depends on the type of anion employed. These transitions are significantly affected by the diffusional efficiencies of the TBA salts to the gel; in other words, once the receptor (gelator) molecules in the gel bind to the anions, the counter TBA cations concertedly approach the anion–receptor complexes to remove the solvent molecules from the entangled fibers and afford the octane solution (Fig. 14c). These transitions in the case of the gel of **13c** are quite distinct from the crystal states mentioned in the former part (e.g., **10d** · Cl$^-$; Fig. 13e), which are due to the insolubility of the TBA salt of **10d** · Cl$^-$ in apolar hydrocarbon solvents. In contrast, the absorption and emission spectra of the gel from **13c** that are changed by the addition of anions suggest that the transitions occur from the molecular assemblies to the dispersed monomeric states. Although intermolecular N–H···F–B

hydrogen bonding may also be essential, this system is a prototypical example of supramolecular gels that use π–π interactions as the main force for aggregation [84]. Thus, anions as additives may not always act as inhibitors but also the building units of soft materials. From this point of view, structural modifications of the anion receptors and the choice of appropriate combinations of anions, cations, receptors, and solvents are currently being investigated in order to harness the fascinating properties of supramolecular gels that are sensitive to chemical stimuli [90]. It seems unsurprising that supramolecular gels, as dimensionally controlled organized structures, consisting of anion receptors can be tuned and modulated by the interactions between anions and binding sites or metal cations that are essential to the formation of gels. However, these observations, which simply exhibit the roles of anions mainly as inhibitors of gel formation, represent the "initial state" in the creation of anion-controllable functional materials. In this context, under the appropriate conditions, various anions can be incorporated into the organized structures as versatile negative-charged building subunits with counter-cationic components.

Solvent-assisted organized structures from amphiphilic anion receptors
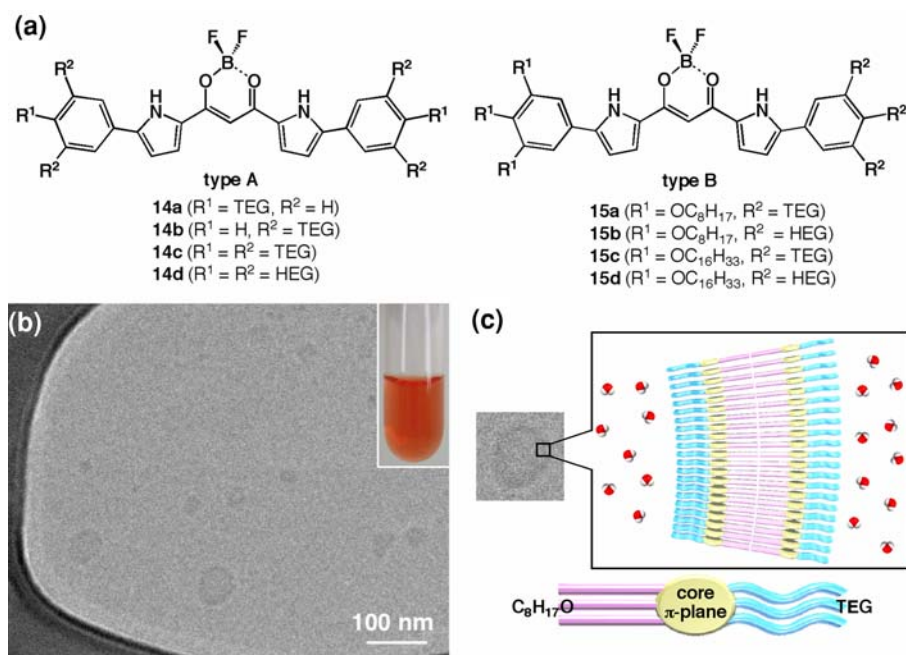
Supramolecular assemblies in an aqueous solution are ubiquitously observed in biotic systems, such as protein folding, DNA double helices, membranes consisting of

lipid bilayers, etc. [129]. These organized structures can be formed by using the interactions between hydrophobic moieties inside the assemblies and the association of hydrophilic sites with water molecules [130, 131]. In artificial systems, various amphiphilic molecules have formed ordered aggregates in the solution state. Among the building subunits for supramolecular assemblies, π-conjugated systems with hydrophilic (and aliphatic) chains are useful for the formation of nanoscale architectures using the stacking of π-planes, which also act as hydrophobic moieties, especially in an aqueous solution. For example, Lee et al. have reported the oligophenylene derivatives and their analogs, which self-assemble to form nanofibers and nanosheets that act as liquid crystals and supramolecular gels as well as micelles and multilayer vesicles [132–137]. Fukushima and Aida et al. have reported that the self-assemblies of amphiphilic hexabenzocoronenes form π-electronic discrete nanotubular objects [138, 139]. Further, Würthner et al. have also reported the morphology control of nanoaggregates depending on the shapes of amphiphilic perylene bisimides [140]. Dynamic conformation changes of the amphiphilic aggregates due to ambient conditions are fascinating from the point of view of their potential applications as soft materials in aqueous solutions. Therefore, organized structures that can be modulated by external physical and chemical stimuli such as temperature, solvents, etc. provide versatile actuators activated in aqueous solutions and related solvents [141–144].

We have synthesized the polyethyleneglycol (PEG)-substituted amphiphilic π-conjugated acyclic oligopyrroles (type A: **14a–d** and type B: **15a–d**, Fig. 15a) by similar procedures for **10a–d** and **13a–c** [84]. These amphiphilic derivatives are soluble in ordinary organic solvents such as CH_2Cl_2, wherein absorption maxima (λ_{max}) of **14a–d** are observed at 519, 503, 517, and 518 nm, respectively, while those of **15a–d** are observed at 519, 520, 519, and 519 nm, respectively. While amphiphiles **14a** and **15c,d** exhibit precipitation in water, the derivatives **14b–d** and **15a,b** are soluble in the same solvent, wherein their λ_{max} values are observed at 460, 496, 506, 462, and 481 nm (1×10^{-5} M), respectively, which are blue-shifted as compared to those in MeOH (498, 510, 512, 510, and 512 nm), suggesting the formation of H-aggregates in aqueous solutions. The absorption spectral changes of **14b–d** and **15a,b** in the mixed solvents of water and miscible MeOH exhibit sweeping "transitions" according to the increasing ratios of water: the sigmoidal curves observed in the transitions between monomers (in MeOH) and assemblies (in water) are due to the selective solvations for each state (monomers and assemblies) by MeOH and water, respectively. As compared to amphiphiles **14b–d** (type A), the stacking interactions of **15a,b** are fairly strong possibly due to the existence of aliphatic long chains, as observed in smaller ratios of water (ca. 30 and 40%) to exhibit blue-shifts. The fluorescence spectra of **14b–d** and **15a,b** in aqueous solutions are observed as each monomer's fluorescence at 546, 571, 572, 672, and 671 nm with the low-emission quantum yields (Φ_F, determined at λ_{ex} values that are equal to the respective λ_{max} values) of 0.01, 0.01, 0.09, 0.02, and 0.02, respectively, which are the characteristic aspects of H-aggregates. This suggestion is also supported by the highly emissive properties of **14b–d** and **15a,b** in MeOH (λ_{em} = 533, 555, 556, 558, and 558 nm; Φ_F = 0.69, 0.37, 0.41, 0.32, and 0.35, respectively) and those in CH_2Cl_2

Fig. 15 (**a**) Amphiphilic derivatives of acyclic anion receptors **14a–d** and **15a–d**; (**b**) Image of cryo-TEM of **15a** from an aqueous solution (1×10^{-5} M) without staining along with the photograph of the aqueous solution (1×10^{-4} M; inset); (**c**) Possible assembling mode of **15a** in vesicles

type A
14a (R^1 = TEG, R^2 = H)
14b (R^1 = H, R^2 = TEG)
14c (R^1 = R^2 = TEG)
14d (R^1 = R^2 = HEG)

type B
15a (R^1 = OC$_8$H$_{17}$, R^2 = TEG)
15b (R^1 = OC$_8$H$_{17}$, R^2 = HEG)
15c (R^1 = OC$_{16}$H$_{33}$, R^2 = TEG)
15d (R^1 = OC$_{16}$H$_{33}$, R^2 = HEG)

(λ_{em} = 534, 558, 559, 564, and 563 nm; Φ_F = 0.94, 0.78, 0.68, 0.81, and 0.73, respectively). DLS measurements of **14b–d** and **15a,b** (1 × 10^{-5} M) in aqueous solutions imply the formation of aggregates with averaged medium sizes around 100–200 nm at 70 °C, while those at 20 °C exhibit fairly random diagrams with larger distributions in **14b–d** and **15a**. The solid films cast from the aqueous solutions of **14b–d** and **15a,b** exhibit almost the same red-shifted UV/vis absorption profiles (λ_{max} = 526, 540, 530, 548, and 531 nm, respectively) as those cast from CH_2Cl_2 solutions, suggesting that the removal of water molecules by slow evaporation at room temperature or by a freeze-drying process disrupts the H-aggregate formations, which are supported by water molecules and instead forming other assembled structures (J-type aggregates).

The morphologies of the transformed organized structures from the aqueous solutions have been examined: only larger assemblies without specific shapes have been observed by TEM analyses of the aqueous solutions (1 × 10^{-5} M) of **14b–d** with $UO_2(OAc)_2$ staining, while under the same conditions, **15a,b** have exhibited the formation of capsules, whose diameters are within the range of 50–150 nm, and cylindrical aggregates, respectively, as the transformed objects by the removal of water molecules around the hydrophilic moieties. The author cannot confirm the extent of the effect of the assembled modes, H- and J-aggregates, on the organized structures as yet, but some insights have been obtained for the speculation of the effect of water-assisted assembled structures. Further, cryo-TEM analysis of **15a** (1 × 10^{-5} M) has also shown the vesicular structures with diameters of 30–80 nm (Fig. 15b), which are consistent with the result of the DLS measurements. The wall thickness (dark part) of capsules is estimated to be ca. 5 nm, which indicates the hydrophobic segments consisting of bilayers of amphiphilic molecules (ca. 3.9 nm by AM1 calculation). Among the organized architectures, vesicles are supramolecular self-assemblies consisting of amphiphiles as the intracellular membrane-enclosed capsules in biotic systems [145–147]. In most cases including the biotic lipids, hydrophilic head groups face toward the water phases in order to maintain hydrophobic tails inside the assemblies. In contrast to the amphiphiles with only hydrophilic chains (type A), possibly, **15a** (type B) forms bilayers like biotic lipids by using hydrophobic interactions of aliphatic chains and locates hydrophilic TEG chains outside the layers to obtain water-soluble vesicles (Fig. 15c). Formation mechanisms and styles of nanoscale structures such as vesicles depend on the molecular structures of the building amphiphiles. Therefore, modifications in the numbers, positions, and shapes of the peripheral substituents will result in versatile, unique organized architectures and stimuli-responsive soft materials with various utilities such as carrier and exciton mobilities [91].

Modifications around boron units of acyclic anion receptors

The replacement of fluorine substituents in a boron moiety of molecular flippers by 1,2-diol units such as catechol derivatives enables the attachment of acyclic anion receptors to the π-conjugated "backbone." We have synthesized catechol-substituted receptors **16a–d** (Fig. 16a) in modest yields from the corresponding dipyrrolyldiketones [79, 81] by treatment with BCl_3 and then with excess catechol derivatives in refluxing CH_2Cl_2. The B–O linkages are fairly stable and therefore the structures of the receptors are maintained during purification by silica gel column chromatography. The UV/vis absorption spectra of "BO_2" complexes **16a** and **16b** in CH_2Cl_2 exhibit the absorption maxima (λ_{max}) at 435 and 454 nm, respectively, which are red-shifted by 2–3 nm in comparison with the maxima of the corresponding BF_2 complexes: unsubstituted **9a** (432 nm) and β-ethyl **9d** (452 nm). Further, compared with the high-intensity fluorescence of **9d** at 471 nm (λ_{em} excited at 420 nm; emission quantum yield: Φ_F = 0.98), the weak fluorescent emission of **16b** observed at 474 nm (λ_{em} excited at 420 nm; Φ_F = 0.026) can be attributed to the quenching path of the intramolecular electron transfer involved in HOMO and HOMO-1, which are localized at the catechol moiety. This observation is consistent with the higher value of Φ_F = 0.82 (λ_{em} = 458 nm excited at 440 nm) of pinacol-substituted analog **16b′**, whose frontier orbitals are localized only at the π-conjugated receptor unit, possibly due to the sp^3 diol moieties. X-ray diffraction analyses of **16a**, **16b**, and **16b′**
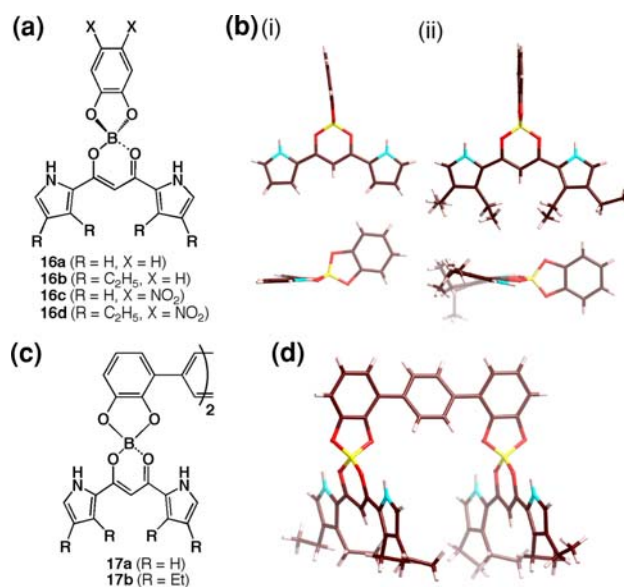

Fig. 16 (a) Catechol-substituted boron complexes of dipyrrolyldiketones **16a–d**; (b) single-crystal X-ray structures of **16a,b** (*top* and *side* view); (c) terphenyl-bridged dimers **17a,b**; (d) single-crystal X-ray structure of **17b**. CCDC#: 684820 (**16a**), 684821 (**16b**), 684823 (**17b**)

have revealed that their structures consist of five-membered rings including two diol oxygens (Fig. 16b). In contrast to **16a** and **16b** with intramolecular N–H···O hydrogen bondings, intriguingly in **16b'**, one of the pyrrole rings is oriented in the opposite direction in the solid state. In a manner similar to BF_2 complexes, the BO_2 complexes **16a**, **16b**, and **16b'** form 1D assembled chain structures by intermolecular interaction between pyrrole NH and catechol oxygens. The binding constants K_a of **16b** (and the ratios to the K_a values of **9d**) for several anions, estimated by the UV/vis absorption spectral changes in CH_2Cl_2 upon the addition of TBA salts, are 2,300 (0.34) (Cl^-), 270 (0.23) (Br^-), 33,000 (0.10) ($CH_3CO_2^-$), 67,000 (0.74) ($H_2PO_4^-$), and 80 (0.07) (HSO_4^-) M^{-1} due to the lower electronegativity of catechol oxygens (**16b**) than that of fluorines (**9d**). The K_a values for anions of **16d** are higher (46,000 (Cl^-), 5400 (Br^-), 1,300,000 ($CH_3CO_2^-$), 150,000 ($H_2PO_4^-$), and 2,300 (HSO_4^-) M^{-1}), due to the effect of electron-withdrawing nitro groups, than those of **16b** in CH_2Cl_2.

The substitution at a boron unit by the vicinal hydroxyl groups of various functional units enables the formation of covalently-linked dimers. The author has synthesized the ditopic receptors **17a** and **17b** (Fig. 16c) by the treatment of intermediate BCl_2 complexes with *p*-phenylene-bridged dicatechol. These receptors are extended systems bridged by "spacer" moieties between the acyclic anion receptor; single-crystal X-ray analysis of **17b** suggests that both the receptor units are oriented in the same direction so that a Π-shaped *syn* conformation is generated with an intramolecular B–B distance of 8.68–9.17 Å (Fig. 16d). Due to the appropriate locations of the two receptor units, **17b** has shown [1+1] binding for linear dicarboxylates ($^-O_2C(CH_2)_nCO_2^-$, $n = 2$–6); the K_a values for succinate ($n = 2$), glutarate ($n = 3$), adipate ($n = 4$), pimelate ($n = 5$), and suberate ($n = 6$) as their TBA salt forms in CH_2Cl_2 are 19,000, 72,000, 810,000, 2,600,000, and 440,000 M^{-1}, respectively. This observation suggests that the distance between the receptor units (ca. 9 Å) is crucial in the determination of the selectivity of the dianions (the DFT-calculated minimum–maximum distances between carboxylate oxygens: 4.90–5.91 Å ($n = 2$), 5.78–7.28 Å ($n = 3$), 7.21–8.58 Å ($n = 4$), 8.05–9.90 Å ($n = 5$), and 9.65–11.22 Å ($n = 6$)). In contrast to the α-linked oligomers [86], the systems based on the BO_2 complexes behave as genuine multitopic receptors that can be incorporated in various macromolecules [92].

Summary and future directions

In this review, the author has demonstrated the recent progress in the supramolecular chemistry of acyclic oligopyrroles, focusing on the works of his group during the last four years. Acyclic oligopyrrole systems have the advantages of exhibiting dynamic conformation changes and more essentially they can be incorporated into various macromolecules and complexes as building subunits by means of covalent and noncovalent interactions such as metal coordination, hydrogen bonding, π–π stacking, etc. At present, the author is attempting to synthesize pyrrole-based π-conjugated molecules that form covalently linked oligomers, supramolecular assemblies, and nanoscale materials, whose conformations and structures can be modulated by external chemical and physical stimuli. In particular, electrostatic hydrogen bonding with anions by π-conjugated acyclic oligopyrroles is fascinating from the view point of forming planar anionic species. The interaction of suitable negative-charged planar units with the appropriate cations will make it possible to form supramolecular assemblies and to tune and control the structures and properties of these materials, thereby making them practical. The use of appropriate molecular design and accurate synthetic procedures for the subunits will allow the formation of soft materials such as gels, liquid crystals, colloids, micelles, etc., consisting of both negative- and positive-charged species as the building components.

References

1. Fischer, H., Orth, H.: Die Chemie des Pyrrols. Akademische Verlagsgesellschaft M. B. H, Leipzig (1934)
2. Kadish, K.M., Smith, K.M., Guilard, R. (eds.): The Porphyrin Handbook. Academic Press, San Diego (2000)

3. Tsoucaris, G. (ed.): Current Challenges on Large Supramolecular Assemblies. NATO Science Series. Kluwer, Dordrecht (1999)

4. Ciferri, A. (ed.): Supramolecular Polymers. Marcel Dekker, New York, Basel (2000)

5. Ozin, G.A., Arsenault, A.C.: Nanochemistry: A Chemical Approach to Nanomaterials. RSC, Cambridge (2005)

6. Würthner, F. (ed.): Supramolecular Dye Chemistry. Topics in Current Chemistry. Springer Verlag, Berlin (2005)

7. Shimizu, T., Matsuda, M., Minamikawa, H.: Supramolecular nanotube architectures based on amphiphilic molecules. Chem. Rev. 105, 1401–1443 (2005). doi:10.1021/cr030072j

8. Hoeben, F.J.M., Jonkheijm, P., Meijer, E.W., Schenning, A.P.H.J.: About supramolecular assemblies of π-conjugated systems. Chem. Rev. 105, 1491–1546 (2005). doi:10.1021/cr030070z

9. Maeda, H.: Supramolecular chemistry of acyclic oligopyrroles. Eur. J. Org. Chem. 5313–5325 (2007), and references therein. doi:10.1002/ejoc.200700382

10. Sauvage, J.-P. (ed.): Transition Metals in Supramolecular Chemistry. Wiley, Chichester (1999)

11. Fujita, M., Umemoto, K., Yoshizawa, M., Fujita, N., Kusukawa, T., Biradha, K.: Molecular paneling via coordination. Chem. Commun. (Camb.) 509–518 (2001). doi:10.1039/b008684n

12. Seidel, S.R., Stang, P.J.: High-symmetry coordination cages via self-assembly. Acc. Chem. Res. 35, 972–983 (2002). doi:10.1021/ar010142d

13. Kitagawa, S., Kitaura, R., Noro, S.: Functional porous coordination polymers. Angew. Chem. Int. Ed. 43, 2334–2375 (2004). doi:10.1002/anie.200300610

14. Dobrawa, R., Würthner, F.: Metallosupramolecular approach toward functional coordination polymers. J. Polym. Sci. A 43, 4981–4995 (2005). doi:10.1002/pola.20997

15. Schubert, U.S., Newkome, G.R., Manners, I. (eds.): Metal-Containing and Metallosupramolecular Polymers and Materials, vol. 928. ACS Symposium Series, American Chemical Society, Washington DC (2006)

16. Oh, M., Mirkin, C.A.: Chemically tailorable colloidal particles from infinite coordination polymers. Nature 438, 651–654 (2005). doi:10.1038/nature04191

17. Oh, M., Mirkin, C.A.: Ion exchange as a way of controlling the chemical compositions of nano- and microparticles made from infinite coordination polymers. Angew. Chem. Int. Ed. 45, 5492–5494 (2006). doi:10.1002/anie.200601918

18. Würthner, F., Stepanenko, V., Sautter, A.: Rigid-rod metallo-supramolecular polymers of dendronized diazadibenzoperylene dyes. Angew. Chem. Int. Ed. 45, 1939–1942 (2006). doi:10.1002/anie.200503717

19. Falk, H.: The Chemistry of Linear and Oligopyrroles and Bile Pigments. Springer-Verlag, Vienna (1989)

20. Brückner, C., Zhang, Y., Rettig, S.J., Dolphin, D.: Synthesis, derivatization and structural characterization of octahedral tris(5-phenyl-4, 6-dipyrrinato) complexes of cobalt(III) and iron(III). Inorg. Chim. Acta 263, 279–286 (1997). doi:10.1016/S0020-1693(97)05700-9

21. Zhang, Y., Thompson, A., Rettig, S.J., Dolphin, D.: The use of dipyrromethene ligands in supramolecular chemistry. J. Am. Chem. Soc. 120, 13537–13538 (1998). doi:10.1021/ja9834982

22. Thompson, A., Rettig, S.J., Dolphin, D.: Self-assembly of novel trimers using dipyrromethene ligands. Chem. Commun. (Camb.) 631–632 (1999). doi:10.1039/a809192g

23. Thompson, A., Dolphin, D.: Nuclear magnetic resonance studies of helical dipyrromethene-zinc complexes. Org. Lett. 2, 1315–1318 (2000). doi:10.1021/ol000053l

24. Chen, Q., Zhang, Y., Dolphin, D.: Synthesis and self-assembly of novel tetra- and hexapyrroles containing dipyrrins linked by a

25. sulfur bridge at the β-position. Tetrahedron Lett. 43, 8413–8416 (2002). doi:10.1016/S0040-4039(02)01958-5

26. Wood, T.E., Thompson, A.: Advances in the chemistry of dipyrrins and their complexes. Chem. Rev. 107, 1831–1861 (2007). doi:10.1021/cr050052c

27. Halper, S.R., Cohen, S.M.: Synthesis, structure, and spectroscopy of phenylacetylenylene rods incorporating meso-substituted dipyrrin ligands. Chem. Eur. J. 9, 4661–4669 (2003). doi:10.1002/chem.200305041

28. Halper, S.R., Cohen, S.M.: Heterometallic metal-organic frameworks based on tris(dipyrrinato) coordination complexes. Inorg. Chem. 44, 486–488 (2005). doi:10.1021/ic048289z

29. Murphy, D.L., Malachowski, M.R., Campana, C.F., Cohen, S.M.: A chiral, heterometallic metal-organic framework derived from a tris(chelate) coordination complex. Chem. Commun. (Camb.) 5506–5508 (2005). doi:10.1039/b510915a

30. Yu, L., Muthukumaran, K., Sazanovich, I.V., Kirmaier, C., Hindin, E., Diers, J.R., Boyle, P.D., Bocian, D.F., Holten, D., Lindsey, J.S.: Excited-state energy-transfer dynamics in self-assembled triads composed of two porphyrins and an intervening Bis(dipyrrinato)metal complex. Inorg. Chem. 42, 6629–6647 (2003). doi:10.1021/ic034559m

31. Maeda, H., Hashimoto, T., Fujii, R., Hasegawa, M.: Dipyrrin Zn^II complexes with functional aryl groups: formation, characterization, and structures in the solid state. J. Nanosci. Nanotechnol. 9, 240–248 (2009). doi:10.1166/jnn.2009.J011

32. Maeda, H., Ito, M.: Dipyrrin-porphyrin hybrids: potential π-conjugated platform to fabricate coordination oligomers. Chem. Lett. 34, 1150–1151 (2005). doi:10.1246/cl.2005.1150

33. Maeda, H., Hasegawa, M., Hashimoto, T., Kakimoto, T., Nishio, S., Nakanishi, T.: Nanoscale spherical architectures fabricated by metal coordination of multiple dipyrrin moieties. J. Am. Chem. Soc. 128, 10024–10025 (2006). doi:10.1021/ja0637301

34. Maeda, H., Hashimoto, T.: Nanoscale metal coordination macrocycles fabricated by using "dimeric" dipyrrins. Chem. Eur. J. 13, 7900–7907 (2007). doi:10.1002/chem.200700444

35. Jeffrey, G.A., Saenger, W.: Hydrogen Bonding in Biological Structures. Springer, Berlin (1991)

36. Whitesides, G.M., Simanek, E.E., Mathias, J.P., Seto, C.T., Chin, D.N., Mannen, M., Gordon, D.M.: Noncovalent synthesis: using physical-organic chemistry to make aggregates. Acc. Chem. Res. 28, 37–44 (1995). doi:10.1021/ar00049a006

37. Prins, L.J., Reinhoudt, D.N., Timmerman, P.: Noncovalent synthesis using hydrogen bonding. Angew. Chem. Int. Ed. 40, 2382–2426 (2001). doi:10.1002/1521-3773(20010702)40:13<2382::AID-ANIE2382>3.0.CO;2-G

38. Ajayaghosh, A., George, S.J., Schenning, A.P.H.J.: Hydrogen-bonded assemblies of dyes and extended π-conjugated systems. In: Würthner, F. (ed.) Supramolecular Dye Chemistry. Topics in Current Chemistry, vol. 258, pp. 83–118. Springer-Verlag, Berlin (2005)

39. Sessler, J.L., Berthon-Gelloz, G., Gale, P.A., Camiolo, S., Anslyn, E.V., Anzenbacher Jr., P., Furuta, H., Kirkovits, G.J., Lynch, V.M., Maeda, H., Morosini, P., Scherer, M., Shriver, J., Zimmerman, R.S.: Oligopyrrole-based solid state self-assemblies. Polyhedron 22, 2963–2983 (2003). doi:10.1016/S0277-5387(03)00436-4

40. Sessler, J.L., Weghorn, S.J., Hiseada, Y., Lynch, V.: Hexaalkyl terpyrrole: a new building block for the preparation of expanded porphyrins. Chem. Eur. J. 1, 56–67 (1995). doi:10.1002/chem.19950010110

41. Scherer, M., Sessler, J.L., Gebauer, A., Lynch, V.: Synthesis and properties of pyrrole-substituted cyclopentadienes. J. Org. Chem. 62, 7877–7881 (1997). doi:10.1021/jo970818b

42. Scherer, M., Sessler, J.L., Moini, M., Gebauer, A., Lynch, V.M.: Self-assembly of pyrrole-ferrocene hybrids, determined inter alia by a new chemically induced electrospray mass spectrometry

technique. Chem. Eur. J. **4**, 152–158 (1998). doi:10.1002/(SICI)1521-3765(199801)4:1<152::AID-CHEM152>3.0.CO;2-E

42. Schmuck, C., Wienand, W.: Highly stable self-assembly in water: ion pair driven dimerization of a guanidiniocarbonyl pyrrole carboxylate zwitterion. J. Am. Chem. Soc. **125**, 452–459 (2003). doi:10.1021/ja028485+

43. Wang, Y., Fu, H., Peng, A., Zhao, Y., Ma, J., Ma, Y., Yao, J.: Distinct nanostructures from isomeric molecules of bis(imino-pyrrole) benzenes: effects of molecular structures on nanostructural morphologies. Chem. Commun. (Camb.) 1623–1625 (2007). doi:10.1039/b701327b

44. Oddo, B., Dainotti, C.: Syntheses in the pyrrole group. V. pyrrolic α-, β- and γ-diketones. Gazz. Chim. Ital. **42**, 716–726 (1912)

45. Stark, W.M., Baker, M.G., Leeper, F.J., Raithby, P.R., Battersby, A.R.: Biosynthesis of porphyrins and related macrocycles. Part 30. Synthesis of the macrocycle of the spiro system proposed as an intermediate generated by cosynthetase. J. Chem. Soc. Perkin Trans. **1**, 1187–1201 (1988). doi:10.1039/p19880001187

46. Maeda, H., Kusunose, Y., Terasaki, M., Ito, Y., Fujimoto, C., Fujii, R., Nakanishi, T.: Micro- and nanometer-scale porous, fibrous, and sheet architectures fabricated by supramolecular assemblies of dipyrrolyldiketones. Chem. Asian J. **2**, 350–357 (2007). doi:10.1002/asia.200600379

47. Maeda, H., Hasegawa, M., Ueda, A.: Hydrogen bonding self-assemblies with 1-D linear, dimeric and hexagonal nanostructures of meso-pyridyl-substituted dipyrromethanes. Chem. Commun. (Camb.) 2726–2728 (2007). doi:10.1039/b703236f

48. Bianchi, A., Bowman-James, K., García-España, E. (eds.): Supramolecular Chemistry of Anions. Wiley-VCH, New York (1997)

49. Singh, R.P., Moyer, B.A. (eds.): Fundamentals and Applications of Anion Separations. Kluwer Academic/Plenum Publishers, New York (2004)

50. Sessler, J.L., Gale, P.A., Cho, W.-S.: Anion Receptor Chemistry. RSC, Cambridge (2006)

51. Vilar, R. (ed.): Recognition of Anions: Structure and Bonding. Springer-Verlag, Berlin (2008)

52. Schmidtchen, F.P., Berger, M.: Signaling recognition events with fluorescent sensors and switches. Chem. Rev. **97**, 1515–1566 (1997). doi:10.1021/cr9603845

53. Beer, P.D., Gale, P.A.: Anion recognition and sensing: the state of the art and future perspectives. Angew. Chem. Int. Ed. **40**, 486–516 (2001). doi:10.1002/1521-3773(20010102)40:3<486::AID-ANIE486>3.0.CO;2-P

54. Sessler, J.L., Camiolo, S., Gale, P.A.: Pyrrolic and polypyrrolic anion binding agents. Coord. Chem. Rev. **240**, 17–55 (2003)

55. Martínez-Máñez, R., Sancenón, F.: Fluorogenic and chromogenic chemosensors and reagents for anions. Chem. Rev. **103**, 4419–4476 (2003). doi:10.1021/cr010421e

56. Gale, P.A.: Amidopyrroles: from anion receptors to membrane transport agents. Chem. Commun. (Camb.) 3761–3772 (2005). doi:10.1039/b504596g

57. Gale, P.A.: Structural and molecular recognition studies with acyclic anion receptors. Acc. Chem. Res. **39**, 465–475 (2006). doi:10.1021/ar040237q

58. Williams, D.H., Cox, J.P.L., Doig, A.J., Gardner, M., Gerhard, U., Kaye, P.T., Lal, A.R., Nicholls, I.A., Salter, C.J., Mitchell, R.C.: Toward the semiquantitative estimation of binding constants. Guides for peptide-peptide binding in aqueous solution. J. Am. Chem. Soc. **113**, 7020–7030 (1991). doi:10.1021/ja00018a047

59. Searle, M.S., Williams, D.H., Gerhard, U.: Partitioning of free energy contributions in the estimation of binding constants: residual motions and consequences for amide–amide hydrogen

bond strengths. J. Am. Chem. Soc. **114**, 10697–10704 (1992). doi:10.1021/ja00053a003

60. Verdejo, B., Aguilar, J., Doménech, A., Miranda, C., Navarro, P., Jiménez, H.R., Soriano, C., García-España, E.: Binuclear Cu^{2+} complex mediated discrimination between L-glutamate and L-aspartate in water. Chem. Commun. (Camb.) 3086–3088 (2005). doi:10.1039/b503417e

61. Gunnlaugsson, T., Kruger, P.E., Jensen, P., Tierney, J., Ali, H.D.P., Hussey, G.M.: Colorimetric "naked eye" sensing of anions in aqueous solution. J. Org. Chem. **70**, 10875–10878 (2005). doi:10.1021/jo0520487

62. Nagai, K., Maeda, K., Takeyama, Y., Sakajiri, K., Yashima, E.: Helicity induction and chiral amplification in a poly(phenylacetylene) bearing N,N-diisopropylaminomethyl groups with chiral acids in water. Macromolecules **38**, 5444–5451 (2005). doi:10.1021/ma0507241

63. Sessler, J.L., Cyr, M.J., Lynch, V., McGhee, E., Ibers, J.A.: Synthetic and structural studies of sapphyrin, a 22-π-electron pentapyrrolic "expanded porphyrin". J. Am. Chem. Soc. **112**, 2810–2813 (1990). doi:10.1021/ja00163a059

64. Shionoya, M., Furuta, H., Lynch, V., Harriman, A., Sessler, J.L.: Diprotonated sapphyrin: a fluoride selective halide anion receptor. J. Am. Chem. Soc. **114**, 5714–5722 (1992). doi:10.1021/ja00040a034

65. Sessler, J.L., Davis, J.: Sapphyrins: versatile anion binding agents. Acc. Chem. Res. **34**, 989–997 (2001). doi:10.1021/ar980117g

66. Gale, P.A., Sessler, J.L., Král, V., Lynch, V.: Calix[4]pyrroles: old yet new anion-binding agents. J. Am. Chem. Soc. **118**, 5140–5141 (1996). doi:10.1021/ja960307r

67. Gale, P.A., Sessler, J.L., Král, V.: Calixpyrroles. Chem. Commun. (Camb.) 1–8 (1998). doi:10.1039/a706280j

68. Sessler, J.L., Gross, D.E., Cho, W.-S., Lynch, V.M., Schmidtchen, F.P., Bates, G.W., Light, M.E., Gale, P.A.: Calix[4]pyrrole as a chloride anion receptor: solvent and counter cation effects. J. Am. Chem. Soc. **128**, 12281–12288 (2006). doi:10.1021/ja064012h

69. Black, C.B., Andrioletti, B., Try, A.C., Ruiperez, C., Sessler, J.L.: Dipyrrolylquinoxalines: efficient sensors for fluoride anion in organic solution. J. Am. Chem. Soc. **121**, 10438–10439 (1999). doi:10.1021/ja992579a

70. Sessler, J.L., Maeda, H., Mizuno, T., Lynch, V.M., Furuta, H.: Quinoxaline-oligopyrroles: improved pyrrole-based anion receptors. Chem. Commun. (Camb.) 862–863 (2002). doi:10.1039/b111708d

71. Sessler, J.L., An, D., Cho, W.-S., Lynch, V., Marquez, M.: Calix[n]bisdipyrrolylbenzenes: synthesis, characterization, and preliminary anion binding studies. Chem. Eur. J. **11**, 2001–2011 (2005). doi:10.1002/chem.200400894

72. Vega, I.E.D., Camiolo, S., Gale, P.A., Hursthouse, M.B., Light, M.E.: Anion complexation properties of 2,2′-bis-amidodipyrrolylmethanes. Chem. Commun. (Camb.) 1686–1687 (2003). doi:10.1039/b303532h

73. Vega, I.E.D., Gale, P.A., Hursthouse, M.B., Light, M.E.: Anion binding properties of 5,5′-dicarboxamido-dipyrrolylmethanes. Org. Biomol. Chem. **2**, 2935–2941 (2004). doi:10.1039/b409115a

74. Vega, I.E.D., Gale, P.A., Light, M.E., Leob, S.J.: NH vs. CH hydrogen bond formation in metal–organic anion receptors containing pyrrolylpyridine ligands. Chem. Commun. (Camb.) 4913–4915 (2005). doi:10.1039/b510506d

75. Schmuck, C.: Side chain selective binding of N-acetyl-α-amino acid carboxylates by a 2-(guanidiniocarbonyl)pyrrole receptor in aqueous solvents. Chem. Commun. (Camb.) 843–844 (1999). doi:10.1039/a901126i

76. Schmuck, C., Geiger, L.: Carboxylate binding by guanidiniocarbonyl pyrroles: from self-assembly to peptide receptors. Curr.

Org. Chem. **7**, 1485–1502 (2003). doi:10.2174/1385272033486387

77. Schmuck, C., Geiger, L.: Efficient complexation of n-acetyl amino acid carboxylates in water by an artificial receptor: unexpected cooperativity in the binding of glutamate but not aspartate. J. Am. Chem. Soc. **127**, 10486–10487 (2005). doi:10.1021/ja052699k

78. Maeda, H., Ito, Y., Kusunose, Y., Nakanishi, T.: Dipyrrolylpyrazoles: anion receptors in protonated form and efficient building blocks for organized structures. Chem. Commun. (Camb.) 1136–1138 (2007). doi:10.1039/b615787d

79. Maeda, H., Kusunose, Y.: Dipyrrolyldiketone difluoroboron complexes: novel anion sensors with C–H···X⁻ interactions. Chem. Eur. J. **11**, 5661–5666 (2005). doi:10.1002/chem.200500627

80. Maeda, H., Terasaki, M., Haketa, Y., Mihashi, Y., Kusunose, Y.: BF₂ complexes of α-alkyl-substituted dipyrrolyldiketones as acyclic anion receptors. Org. Biomol. Chem. **6**, 433–436 (2008). doi:10.1039/b718317h

81. Maeda, H., Kusunose, Y., Mihashi, Y., Mizoguchi, T.: BF₂ complexes of β-tetraethyl-substituted dipyrrolyldiketones as anion receptors: potential building subunits for oligomeric systems. J. Org. Chem. **72**, 2616–2621 (2007). doi:10.1021/jo062660d

82. Maeda, H., Ito, Y.: BF₂ complex of fluorinated dipyrrolyldiketone: a new class of efficient receptor for acetate anions. Inorg. Chem. **45**, 8205–8210 (2006). doi:10.1021/ic0608703

83. Fujimoto, C., Kusunose, Y.: CH···anion interaction in BF₂ complexes of C₃-bridged oligopyrroles. H. Maeda. J. Org. Chem. **71**, 2389–2394 (2006). doi:10.1021/jo052511f

84. Maeda, H., Haketa, Y., Nakanishi, T.: Aryl-substituted C₃-bridged oligopyrroles as anion receptors for formation of supramolecular organogels. J. Am. Chem. Soc. **129**, 13661–13674 (2007). doi:10.1021/ja074435z

85. Maeda, H., Eifuku, N.: Receptors with mono-alkoxy-substituted aryl rings have also been synthesized: Alkoxy-substituted derivatives of π-conjugated acyclic anion receptors: effects of substituted positions. Chem. Lett. **38**, 208–209 (2009). doi:10.1246/cl.2009.208

86. Maeda, H., Haketa, Y.: Selective iodinated dipyrrolyldiketone BF₂ complexes as potential building units for oligomeric systems. Org. Biomol. Chem. **6**, 3091–3095 (2008). doi:10.1039/b806161k

87. Maeda, H., Mihashi, Y., Haketa, Y.: Heteroaryl-substituted C₃-bridged oligopyrroles: potential building subunits of anion-responsive π-conjugated oligomers. Org. Lett. **10**, 3179–3182 (2008). doi:10.1021/ol801014z

88. Maeda, H., Bando, Y., Haketa, Y., Seki, S., Tohnai, N.: Recently, we have found the formation of multicrystalline systems of **9a**. (to be submitted)

89. Maeda, H., Haketa, Y., Bando, Y., Sakamoto, S.: For single-crystal structures of β-ethyl-substituted receptor **9d**: Synthesis, properties, and solid-state assemblies of β-alkyl-substituted dipyrrolyldiketone BF₂ complexes. Synth. Met. **159** (2009). doi:10.1016/j.synthmet.2009.01.004

90. Maeda, H., Haketa, Y., Terashima, Y., Shimosugi, S., Ohta, K.: Effects of counter cations have also been examined. (to be submitted)

91. Maeda, H., Ito, Y., Haketa, Y., Eifuku, N., Lee, E., Lee, M., Hashishin, T., Kaneko, K.: Solvent-assisted organized structures based on amphiphilic anion-responsive π-conjugated systems. Chem. Eur. J. **15**, (2009). doi:10.1002/chem.200802152

92. Maeda, H., Fujii, Y., Mihashi, Y.: Diol-substituted boron complexes of dipyrrolyl diketones as anion receptors and covalently linked 'pivotal' dimers. Chem. Commun. (Camb.) 4285–4287 (2008). doi:10.1039/b806361c

93. Sanchez-Queseda, J., Seel, C., Prados, P., de Mendoza, J.: Anion helicates: double strand helical self-assembly of chiral bicyclic guanidinium dimers and tetramers around sulfate templates. J. Am. Chem. Soc. **118**, 277–278 (1996). doi:10.1021/ja953243d

94. Keegan, K., Kruger, P.E., Nieuwenhuyzen, M., O'Brien, J., Martin, N.: Anion directed assembly of a dinuclear double helicate. Chem. Commun. (Camb.) 2192–2193 (2001). doi:10.1039/b106981k

95. Coles, S.J., Frey, J.G., Gale, P.A., Hursthouse, M.B., Light, M.E., Navakhun, K., Thomas, G.L.: Anion-directed assembly: the first fluoride-directed double helix. Chem. Commun. (Camb.) 568–569 (2003). doi:10.1039/b210847j

96. Coles, S.J., Gale, P.A., Hursthouse, M.B., Light, M.E., Warriner, C.N.: Crystallographic and solution anion binding studies of bis-amidofurans and thiophenes. Supramol. Chem. **16**, 469–486 (2004). doi:10.1080/10610270410001713303

97. Curiel, D., Cowley, A., Beer, P.D.: Indolocarbazoles: a new family of anion sensors. Chem. Commun. (Camb.) 236–238 (2005). doi:10.1039/b412363h

98. Brook, S.J., Evans, L.S., Gale, P.A., Hursthouse, M.B., Light, M.E.: 'Twisted' isophthalamide analogues. Chem. Commun. (Camb.) 734–735 (2005). doi:10.1039/b413654c

99. Gale, P.A., Light, M.E., McNally, B., Navakhun, K., Sliwinski, K.E., Smith, B.D.: Co-transport of H⁺/Cl⁻ by a synthetic prodigiosin mimic. Chem. Commun. (Camb.) 3773–3775 (2005). doi:10.1039/b503906a

100. Hirose, J., Inoue, K., Sakuragi, H., Kikkawa, M., Minakami, M., Morikawa, T., Iwamoto, H., Hiromi, K.: Anions binding to bilirubin oxidase from *Trachyderma tsunodae* K-2593. Inorg. Chim. Acta **273**, 204–212 (1998). doi:10.1016/S0020-1693(97)06183-5

101. Sato, M., Kanamori, T., Kamo, N., Demura, M., Nitta, K.: Stopped-flow analysis on anion binding to blue-form halorhodopsin from *Natronobacterium pharaonis*: comparison with the anion-uptake process during the photocycle. Biochemistry **41**, 2452–2458 (2002). doi:10.1021/bi011788g

102. Swager, T.M.: Semiconducting Poly(arylene ethylene)s. In: Diederich, F., Stang, P.J., Tykwinski, R.R. (eds.) Acetylene Chemistry. Wiley-VCH, New York (2005). (Chap. 6)

103. McQuade, D.T., Pullen, A.E., Swager, T.M.: Conjugated polymer-based chemical sensors. Chem. Rev. **100**, 2537–2574 (2000). doi:10.1021/cr9801014

104. Rose, A., Zhu, Z., Madigan, C.F., Swager, T.M., Bulovi'c, V.: Sensitivity gains in chemosensing by lasing action in organic polymers. Nature **434**, 876–879 (2005). doi:10.1038/nature03438

105. Fages, F. (ed.): Low Molecular Mass Gelators, vol. 256, p. 283. Topics in Current Chemistry. Springer-Verlag, Berlin (2005)

106. Ishi-i, T., Shinkai, S.: Dye-Based Organogels: Stimuli-Responsive Soft Materials Based on One-Dimensional Self-Assembling Aromatic Dyes. In: Würthner, F. (ed.) Supramolecular Dye Chemistry. Topics in Current Chemistry, vol. 258, pp. 119–160. Springer-Verlag, Berlin (2005)

107. Terech, P., Weiss, R.G.: Low molecular mass gelators of organic liquids and the properties of their gels. Chem. Rev. **97**, 3133–3159 (1997). doi:10.1021/cr9700282

108. Abdallah, D.J., Weiss, R.G.: Organogels and low molecular mass organic gelators. Adv. Mater. **12**, 1237–1247 (2000). doi:10.1002/1521-4095(200009)12:17<1237::AID-ADMA1237>3.0.CO;2-B

109. Kato, T., Mizoshita, N., Kishimoto, K.: Functional liquid-crystalline assemblies: self-organized soft materials. Angew. Chem. Int. Ed. **45**, 38–68 (2006). doi:10.1002/anie.200501384

110. van Esch, J.H., Feringa, B.L.: New functional materials based on self-assembling organogels: from serendipity towards design.

Angew. Chem. Int. Ed. **39**, 2263–2266 (2000). doi:10.1002/1521-3773(20000703)39:13<2263::AID-ANIE2263>3.0.CO;2-V

111. Kawano, S.-i., Tamaru, S.-i., Fujita, N., Shinkai, S.: Sol-gel polycondensation of tetraethyl orthosilicate (TEOS) in sugar-based porphyrin organogels: inorganic conversion of a sugar-directed porphyrinic fiber library through Sol-gel transcription processes. Chem. Eur. J. **10**, 343–351 (2004). doi:10.1002/chem.200305042

112. Shirakawa, M., Fujita, N., Shinkai, S.: A stable single piece of unimolecularly π-stacked porphyrin aggregate in a thixotropic low molecular weight gel: a one-dimensional molecular template for polydiacetylene wiring up to several tens of micrometers in length. J. Am. Chem. Soc. **127**, 4164–4165 (2005). doi:10.1021/ja042869d

113. Kitahara, T., Shirakawa, M., Kawano, S.-i., Beginn, U., Fujita, N., Shinkai, S.: Creation of a mixed-valence state from one-dimensionally aligned ttf utilizing the self-assembling nature of a low molecular-weight gel. J. Am. Chem. Soc. **127**, 14980–14981 (2005). doi:10.1021/ja0552038

114. Yagai, S., Nakajima, T., Kishikawa, K., Kohmoto, S., Karatsu, T., Kitamura, A.: Hierarchical organization of photoresponsive hydrogen-bonded rosettes. J. Am. Chem. Soc. **127**, 11134–11139 (2005). doi:10.1021/ja052645a

115. Maeda, H.: Recently, the author has summarized the recent progress of the anion-responsive supramolecular gels: Anion-responsive supramolecular gels. Chem. Eur. J. **14**, 11274–11282 (2008). doi:10.1002/chem.200801333

116. Balaban, T.S., Tamiaki, H., Holzwarth, A.R.: Chlorins Programmed for Self-Assembly. In: Würthner, F. (ed.) Supramolecular Dye Chemistry. Topics in Current Chemistry, vol. 258, pp. 1–38. Springer-Verlag, Berlin (2005)

117. Webb, J.E.A., Crossley, M.J., Turner, P., Thordarson, P.: Pyromellitamide aggregates and their response to anion stimuli. J. Am. Chem. Soc. **129**, 7155–7162 (2007). doi:10.1021/ja0713781

118. Džolić, Z., Cametti, M., Cort, A.D., Mandolini, L., Žinić, M.: Fluoride-responsive organogelator based on oxalamide-derived anthraquinone. Chem. Commun. (Camb.) 3535–3537 (2007). doi:10.1039/b707466b

119. Wang, C., Zhang, D., Zhu, D.: A chiral low-molecular-weight gelator based on binaphthalene with two urea moieties: modulation of the CD spectrum after gel formation. Langmuir **23**, 1478–1482 (2007). doi:10.1021/la062621x

120. Yang, H., Yi, T., Zhou, Z., Zhou, Y., Wu, J., Xu, M., Li, F., Huang, C.: Switchable fluorescent organogels and mesomorphic superstructure based on naphthalene derivatives. Langmuir **23**, 8224–8230 (2007). doi:10.1021/la7005919

121. Yamanaka, M., Nakamura, T., Nakagawa, T., Itagaki, H.: Reversible sol–gel transition of a tris–urea gelator that responds to chemical stimuli. Tetrahedron Lett. **48**, 8990–8993 (2007). doi:10.1016/j.tetlet.2007.10.090

122. Stanley, C.E., Clarke, N., Anderson, K.M., Elder, J.A., Lenthall, J.T., Steed, J.W.: Anion binding inhibition of the formation of a helical organogel. Chem. Commun. (Camb.) 3199–3201 (2006). doi:10.1039/b606373j

123. Piepenbrock, M.-O.M., Lloyd, G.O., Clarke, N., Steed, J.W.: Gelation is crucially dependent on functional group orientation and may be tuned by anion binding. Chem. Commun. (Camb.) 2644–2646 (2008). doi:10.1039/b804259d

124. Applegarth, L., Clark, N., Richardson, A.C., Parker, A.D.M., Radosavljevic-Evans, I., Goeta, A.E., Howard, J.A.K., Steed, J.W.: Modular nanometer-scale structuring of gel fibres by sequential self-organization. Chem. Commun. (Camb.) 5423–5425 (2005). doi:10.1039/b511259a

125. Li, Q., Wang, Y., Li, W., Wu, L.: Structural characterization and chemical response of a Ag-coordinated supramolecular gel. Langmuir **23**, 8217–8223 (2007). doi:10.1021/la700364t

126. Kishimura, A., Yamashita, T., Aida, T.: Phosphorescent organogels via "Metallophilic" interactions for reversible RGB-color switching. J. Am. Chem. Soc. **127**, 179–183 (2005). doi:10.1021/ja0441007

127. Kim, H.-J., Zin, W.-C., Lee, M.: Anion-directed self-assembly of coordination polymer into tunable secondary structure. J. Am. Chem. Soc. **126**, 7009–7014 (2004). doi:10.1021/ja049799v

128. Kim, H.-J., Lee, J.-H., Lee, M.: Stimuli-responsive gels from reversible coordination polymers. Angew. Chem. Int. Ed. **44**, 5810–5814 (2005). doi:10.1002/anie.200501270

129. Voet, D., Voet, J.G.: Biochemistry. Wiley, New York (2004)

130. Israelachvili, J.N.: Intermolecular and Surface Forces, p. 450. Academic Press, London (1992)

131. Hamley, I.W.: Introduction to Soft Matter–Polymers, Colloids, Amphiphiles and Liquid Crystals, p. 342. Wiley, Chichester (2000)

132. Lee, M., Jeong, Y.-S., Cho, B.-K., Oh, N.-K., Zin, W.-C.: Self-assembly of molecular dumbbells into organized bundles with tunables size. Chem. Eur. J. **8**, 876–883 (2002). doi:10.1002/1521-3765(20020215)8:4<876::AID-CHEM876>3.0.CO;2-M

133. Yoo, Y.-S., Choi, J.-H., Song, J.-H., Oh, N.-K., Zin, W.-C., Park, S., Chang, T., Lee, M.: Self-assembling molecular trees containing octa-p-phenylene: from nanocrystals to nanocapsules. J. Am. Chem. Soc. **126**, 6294–6300 (2004). doi:10.1021/ja048856h

134. Jin, L.-Y., Ahn, J.-H., Lee, M.: Shape-persistent macromolecular disks from reactive supramolecular rod bundles. J. Am. Chem. Soc. **126**, 12208–12209 (2004). doi:10.1021/ja0465552

135. Hong, D.-J., Lee, E., Lee, M.: Nanofibers from self-assembly of an aromatic facial amphiphile with oligo(ethylene oxide) dendrons. Chem. Commun. (Camb.) 1801–1803 (2007). doi:10.1039/b617404c

136. Moon, K.-S., Kim, H.-J., Lee, E., Lee, M.: Self-assembly of T-shaped aromatic amphiphiles into stimulus-responsive nanofibers. Angew. Chem. Int. Ed. **46**, 6807–6810 (2007). doi:10.1002/anie.200702136

137. Lee, E., Jeong, Y.-H., Kim, J.-K., Lee, M.: Controlled self-assembly of asymmetric dumbbell-shaped rod amphiphiles: transition from toroids to planar nets. Macromolecules **40**, 8355–8360 (2007). doi:10.1021/ma071511+

138. Hill, J.P., Jin, W., Kosaka, A., Fukushima, T., Ichihara, H., Shimomura, T., Ito, K., Hashizume, T., Ishii, N., Aida, T.: Self-assembled hexa-peri-hexabenzocoronene graphitic nanotube. Science **304**, 1481–1483 (2004). doi:10.1126/science.1097789

139. Yamamoto, Y., Fukushima, T., Suna, Y., Ishii, N., Saeki, A., Seki, S., Tagawa, S., Taniguchi, M., Kawai, T., Aida, T.: Photoconductive coaxial nanotubes of molecularly connected electron donor and acceptor layers. Science **314**, 1761–1764 (2006). doi:10.1126/science.1134441

140. Zhang, X., Chen, Z., Würthner, F.: Morphology control of fluorescent nanoaggregates by co-self-assembly of wedge- and dumbbell-shaped amphiphilic perylene bisimides. J. Am. Chem. Soc. **129**, 4886–4887 (2007). doi:10.1021/ja070994u

141. McCormick, C.L. (ed.): Stimuli-Responsive Water Soluble and Amphiphilic Polymers. ACS, Washington, DC (2001)

142. Urban, M.W. (ed.): Stimuli-Responsive Polymeric Films and Coating. ACS, Washington, DC (2005)

143. Aathimanikandan, S.V., Savariar, E.N., Thayumanavan, S.: Temperature-sensitive dendritic micelles. J. Am. Chem. Soc. **127**, 14922–14929 (2005). doi:10.1021/ja054542y

144. Basu, S., Vutukuri, D.R., Thayumanavan, S.: Homopolymer micelles in heterogeneous solvent mixtures. J. Am. Chem. Soc. **127**, 16794–16795 (2005). doi:10.1021/ja056042a

145. Luisi, P.L., Walde, P. (eds.): Giant Vesicles. Wiley-VCH, Chichester (2000)

146. Shioi, A., Hatton, T.A.: Model for formation and growth of vesicles in mixed anionic/cationic (SOS/CTAB) surfactant systems. Langmuir **18**, 7341–7348 (2002). doi:10.1021/la020268z

147. Li, Z., Hillmyer, M.A., Lodge, T.P.: Laterally nanostructured vesicles, polygonal bilayer sheets, and segmented wormlike micelles. Nano Lett. **6**, 1245–1249 (2006). doi:10.1021/nl0608700